Title 論文題目	Self-renewal capability of hepatocytic parental progenitor cells derived from adult rat liver is maintained long term when cultured on laminin 111 in serum-free medium （成体ラット由来の肝親前駆細胞の自己複製能は無血清培地を用いたラミニン 111 上での培養により長期間維持される）
Author(s) 著　者	木野, 潤一
Degree number 学位記番号	甲第 3076 号
Degree name 学位の種別	博士（医学）
Issue Date 学位取得年月日	2020-03-31
Original Article 原著論文	Hepatology Communications. 2019; in press.
Doc URL	
DOI	
Resource Version	Publisher Edition

HEPATOLOGY COMMUNICATIONS, VOL. 0, NO. 0, 2019

Self-Renewal Capability of Hepatocytic Parental Progenitor Cells Derived From Adult Rat Liver Is Maintained Long Term When Cultured on Laminin 111 in Serum-Free Medium

Junichi Kino,[1,2*] Norihisa Ichinohe,[1*] Masayuki Ishii,[1,3] Hiromu Suzuki,[4] Toru Mizuguchi,[3] Naoki Tanimizu,[1] and Toshihiro Mitaka [1]

In this study, we investigated how the ability of hepatocytic parental progenitor cells (HPPCs) to self-renew can be maintained and how laminin (LN) isoforms play an important role in their self-renewal and maturation. Hepatocytes isolated from adult rat livers were cultured on hyaluronic acid to form colonies consisting of $CD44^+$ small hepatocytes, which could be passaged on dishes coated with Matrigel. When second-passage cells were plated on Matrigel, LN111, or LN511, HPPCs appeared on Matrigel and LN111 but not on LN511. We identified two types of cells among the second-passage cells: Small, round cells and large, flat ones were observed on Matrigel, whereas the former and latter ones were specifically attached on LN111 and LN511, respectively. We hypothesized that small and round cells are the origin of HPPC colonies, and the binding to LN111 could be key to maintaining their self-renewal capability. Among the integrins involved in LN binding, integrins α3 and β1 were expressed in colonies on LN111 more than in those on LN511, whereas β4 was more strongly expressed in colonies on LN511. Integrin $\alpha3^{high}\alpha6\beta1^{high}$ cells could form HPPC colonies on LN111 but not on LN511, whereas integrin $\alpha6\beta1^{low}$ cells could not on either LN111 or LN511. In addition, neutralizing anti-integrin β1 and anti-LN111 antibodies inhibited the passaged cells' ability to attach and form colonies on LN111 by HPPCs. Matrigel overlay induced second-passage cells growing on LN111 to increase their expression of hepatic functional genes and to form 3-dimensional colonies with bile canalicular networks, whereas such a shift was poorly induced when they were grown onLN511. *Conclusion:* These results suggest that the self-renewal capability of HPPCs depends on LN111 through integrin β1 signaling. (*Hepatology Communications* 2019;0:1-17).

Whole or segmental liver transplantation is widely chosen as the last option to save patients suffering from severe liver diseases, yet a persistent shortage of donor organs prevents most patients from receiving the benefits of transplantation. Thus, cell-based therapies, such as

Abbreviations: 3D, 3-dimensional; Ab, antibody; ALB, albumin; ANOVA, analysis of variance; BC, bile canaliculi; BM, basement membrane; C/EBPα, CCAAT/enhancer binding protein α; ECM, extracellular matrix; FACS, fluorescence-activated cell sorting; FD, fluorescein diacetate; HA, hyaluronic acid; HiPSC, human-induced PSC; HNF, hepatocyte nuclear factor; HPPC, hepatocytic parental progenitor cell; ICAM-1, intercellular cell adhesion molecule-1; Itg, integrin; LN, laminin; MGOL, Matrigel overlay; MH, mature hepatocyte; PCR, polymerase chain reaction; PSC, pluripotent stem cell; qRT-PCR, quantitative reverse-transcription PCR; SC, satellite cell; SH, small hepatocyte.

Received April 16, 2019; accepted October 7, 2019.

Additional Supporting Information may be found at onlinelibrary.wiley.com/doi/10.1002/hep4.1442/suppinfo.

Supported by the Ministry of Education, Culture, Sports, Science, and Technology, Japan (17K08765, 17K10672, 17K19703, and 18H02873).

**These authors contributed equally to this work.*

View this article online at wileyonlinelibrary.com.

DOI 10.1002/hep4.1442

Potential conflict of interest: Dr. Kino and his spouse are employed by Otsuka and Novartis, respectively.

cell transplantation, engineered hepatocellular tissue constructs, and bio-artificial liver devices, have been considered as alternatives to whole-liver transplantation.[1-3] A large number of healthy hepatocytes are required for these therapies to compensate for their insufficient hepatic function. However, it is quite difficult to routinely obtain healthy human hepatocytes because of severe liver donor shortages and a lack of methods to expand functional hepatocytes.

Small hepatocytes (SHs) are a subpopulation of mature hepatocytes (MHs) that can act as hepatocytic progenitor cells.[4,5] Importantly, approximately 2.5% of MHs in young adult rat liver have the potential to become SHs, and this proportion gradually decreases with age.[6] Rat and human SHs can proliferate to form colonies in serum-free medium when cultured on hyaluronic acid (HA)-coated dishes.[7,8] In addition, SHs consistently and specifically express CD44, an HA receptor.[9] We recently reported that hepatocytic parental progenitor cells (HPPCs) exist among $CD44^+$ SHs.[10] HPPCs continue to proliferate and generate daughter cells after passages, which indicates that they possess the ability to self-renew. In fact, rat HPPCs can potentially divide more than 50 times in a period of 17 weeks and over four passages. Although primary SHs require HA to attach to and grow on, under serum-free conditions, most passaged cells do not attach to HA-coated dishes. On the other hand, HPPCs were reported to expand on dishes coated with Matrigel derived from Engelbreth–Holm–Swarm sarcoma and containing components of basement membrane (BM)[11]; this suggests that Matrigel's extracellular matrix (ECM) component is crucial for HPPCs to maintain their ability to self-renew.

Adhesive interactions of epithelial cells with underlying BM are known to be instrumental for the development, differentiation, and maintenance of tissues. The major components of BM are laminins (LNs), type IV collagen, nidogen, and heparan sulfate proteoglycans.[12] Among these components, LNs serve as the major adhesive proteins and mediate the adhesion of cells to BM. LNs are composed of three polypeptide chains, designated as α, β, and γ, and five α (α1-5), three β (β1-3), and three γ (γ1-3) chains are recognized in mammals.[13] Matrigel contains LN111(α1, β1, γ1) as a major constituent.[11] The LNα1-chain is expressed in fetal and early-adult rat liver lobules but is not found in mature adults; instead, the LN α5-chain is present in the portal triads.[14] However, the transient expression of LNα1 has been observed in regenerating liver after partial hepatectomy.[14] Integrins play central roles in the adhesion of cells to LNs.[13] They are composed of noncovalently associated α and β subunits. To date, at least 24 separate integrins consisting of distinct combinations of α and β subunits have been identified in mammals. Among these, integrins α3β1, α6β1, α6β4, and α7β1 function as major LN-binding receptors.[12] The specificity of LN–integrin interaction is dependent primarily on LN α-chains, and the integrin ligand specificity is determined primarily by the α subunits. Integrin β subunits play an auxiliary role in the specificity.[12,13]

Preliminary experiments have shown that only 15% to 20% of $CD44^+$ SHs attach to LN111-coated or Matrigel-coated dishes, although more than 40% attach to LN511-coated ones.[10] In the present study, we investigated how HPPCs' self-renewal capability can be maintained and how LN isoforms play a role

ARTICLE INFORMATION:

From the [1]Department of Tissue Development and Regeneration, Research Institute for Frontier Medicine, Sapporo Medical University School of Medicine, Sapporo, Japan; [2]Medical Regulatory Affairs Department, Otsuka Pharmaceutical Co. Ltd, Tokyo, Japan; [3]Department of Surgery, Surgical Oncology and Science; [4]Department of Molecular Biology, Sapporo Medical University School of Medicine, Sapporo, Japan.

ADDRESS CORRESPONDENCE AND REPRINT REQUESTS TO:

Toshihiro Mitaka, M.D., Ph.D.
Department of Tissue Development and Regeneration
Research Institute for Frontier Medicine
Sapporo Medical University School of Medicine
South-1, West-17
Chuo-ku, Sapporo 060-8556, Japan
E-mail: tmitaka@sapmed.ac.jp
Tel.: +81-11-688-9615

in their self-renewal and maturation. Although a population of HPPCs maintains a smaller size and the ability to self-renew, cells that have a large cytoplasm and lose the ability to self-renew can also be generated. Among integrins involved in LN binding, integrins α3 and β1 were expressed in colonies on LN111 more than in those on LN511, whereas β4 was more strongly expressed in colonies on LN511. Integrin $\alpha3^{high}\alpha6\beta1^{high}$ but not $\alpha6\beta1^{low}$ cells could form HPPC colonies on LN111 but not on LN511. In addition, both neutralizing anti-integrin β1 and anti-LN111 antibodies inhibited the cells' attachment to LN111 as well as colony formation by HPPCs. These results suggest that HPPCs' self-renewal capability depends on LN111 through integrin β1 signaling. Furthermore, Matrigel overlay (MGOL) induced second-passage cells growing on LN111 to increase the expression of hepatic functional genes and to form 3-dimensional (3D) colonies with bile canalicular networks, whereas such a shift was poorly induced when they were grown on LN511. Thus, HPPCs' abilities to self-renew and mature depend on LN111.

Materials and Methods

ANIMALS

Six-week-old to 10-week-old male F344 rats (dipeptidylpeptidase IV^+ strain; Sankyo Lab Service Corporation, Inc., Tokyo, Japan) were used for cell isolation. The animals were kept at a constant temperature of 23°C ± 1°C under a 12-hour light/dark cycle with standard chow and water *ad libitum*. The experimental protocol was approved by the Committee on Laboratory Animals and complied with Sapporo Medical University guidelines (Approval Nos. 13-132 and 13-134).

CELL ISOLATION, CULTURE, AND PASSAGES

Primary SHs were isolated by the collagenase perfusion method, as described.[7] The details of the methods for cell culture and passage have been reported.[10] In the experiments using LNs, second-passage cells were plated on 12-well plates coated with LN111, LN511, LN521, and Matrigel (see Supporting Information for details). The medium was replaced every other day, and the cells were passaged every 4 weeks.

ADHESIVE PROPERTIES OF PASSAGED CELLS TO LNs

To examine whether two different populations are generated during the culture of passaged cells, first-passage cells, which had been cultured on Matrigel-coated dishes for 21 days, were collected by trypsinization and plated onto LN111-coated 35-mm dishes. Three hours after plating, culture medium containing unattached cells was collected and transferred to LN511-coated 35-mm dishes. The medium was replenished for the cells on LN111, and 1 hour later, all cells on LN111, LN511, and Matrigel were harvested. The collected cells were used for gene-expression analysis using oligo microarrays and quantitative reverse-transcription polymerase chain reaction (qRT-PCR) (see Supporting Information for details).

MORPHOLOGICAL ANALYSES OF CULTURED CELLS

Colonies were photographed with a phase-contrast microscope equipped with a charge-coupled device camera (Olympus Optical Co., Tokyo, Japan) to assess the number of colonies, the number of cells per colony, and the sizes of cells and colonies. At least 10 fields per dish or well were randomly selected, and three dishes or wells were examined per experiment. At least two independent experiments were performed. All captured images were processed using specialized software (Olympus cellSens Dimension Desktop 1.12; Olympus Optical Co.).

COMPREHENSIVE GENE ANALYSIS AND PCR

Differences in gene expression related to hepatic functions and stem cell properties among the cells attached to LN111, LN511, and Matrigel were analyzed using an oligo microarray spotted with 30,584 probes (SurePrint G3 Rat Gene Expression v2 G4853B; Agilent Technologies, Santa Clara, CA) and by qRT-PCR (see Supporting Information for details).

FLUORESCENT IMMUNOCYTOCHEMISTRY

For details on the fluorescent immunocytochemistry, see the Supporting Information.

MEASURING LABELING INDEX

The cells were treated with 40 μM 5-bromo-2′-deoxyuridine (BrdU) at 18 hours before fixation and the immunocytochemistry for BrdU (see Supporting Information for details).

FLOW CYTOMETRY

First-passage cells, cultured on the Matrigel-coated dishes for 28 days, were collected and incubated with mouse antirat integrin α6β1 or goat antirat integrin α3 antibodies in Dulbecco's modified Eagle's medium/F12 medium containing 10% fetal bovine serum for 30 minutes at 4°C. Integrin $\alpha3^{high}\alpha6\beta1^{high}$, $\alpha3^{low}\alpha6\beta1^{high}$, or $\alpha3^{low}\alpha6\beta1^{low}$ cells were sorted using a fluorescence-activated cell sorting (FACS) Aria cell sorter (BD Biosciences, San Jose, CA) and plated onto LN111-coated, LN511-coated, and Matrigel-coated 12-well plates. Data were analyzed using Kaluza Flow Cytometry Software version 1.1 (Beckman Coulter, Inc., Brea, CA) (see Supporting Information for details).

INHIBITION ASSAY BY NEUTRALIZING ANTIBODIES

First-passage cells, cultured on Matrigel-coated dishes for 28 days, were collected by trypsinization. To study integrin β1 and LN111 dependence, neutralizing antibodies against integrin β1 and LN111 were used, respectively (see Supporting Information for details).

MATURATION OF HPPCs BY MGOL

First-passage cells, cultured on Matrigel for 28 days, were separated and plated on LN111-coated, LN511-coated, and Matrigel-coated dishes. The cells were cultured for 14 days and then either overlaid with Matrigel or untreated and then cultured for an additional 7 days. To assess the formation of bile canaliculi (BC), the cells were incubated for 30 minutes following the addition of 0.25% fluorescein diacetate (FD) (Sigma-Aldrich Co., St Louis, MO) to the medium and then rinsed 3 times with phosphate-buffered saline (PBS). Fluorescent images were immediately taken using a phase-contrast microscope equipped with a fluorescence device (Olympus Optical, Co.). Gene expression by these cells was analyzed by qRT-PCR.

SCANNING ELECTRON MICROSCOPY

To observe the morphology of cells initially attached on LN111-coated, LN511-coated, and Matrigel-coated dishes, the cells were fixed in PBS containing 2.5% glutaraldehyde solution (see Supporting Information for details).

STATISTICAL ANALYSIS

All data were analyzed using analysis of variance (ANOVA) with Tukey's multiple comparison test or Kruskal–Wallis with Dunn's multiple comparison test. Experimental results are expressed as the geometric mean ± SEM.

Results

We first confirmed our preliminary results.[10] First-passage cells were plated on dishes coated with ECMs, including LN-α1 (LN111 and Matrigel) or α5 (LN511 and LN521). The adhesion rates of cells on day 1 were 15% to 20% and 40% to 50% on LN111 and LN511/521, respectively (data not shown), which was consistent with our preliminary results.[10] The sizes of the attached cells on day 1 were measured, and those on LN511/521 were significantly larger than those on LN111 (Supporting Fig. S2A). Moreover, the features of cells on each ECM differed quite markedly in the early period after plating (Fig. 1 and Supporting Fig. S2B). At 3 hours, most cells attached to LN511/521 rapidly spread their cytoplasm to produce flattened features, whereas those on LN111 retained their spherical shapes. The different features of cells on each ECM were maintained even at day 1. Both types of cell that appeared on LN111 and LN511/521 were observed on Matrigel (Fig. 1A). Scanning electron microscopy revealed fine structures of cells on LN111, LN511, and Matrigel at day 1 (Fig. 1B). Cells on

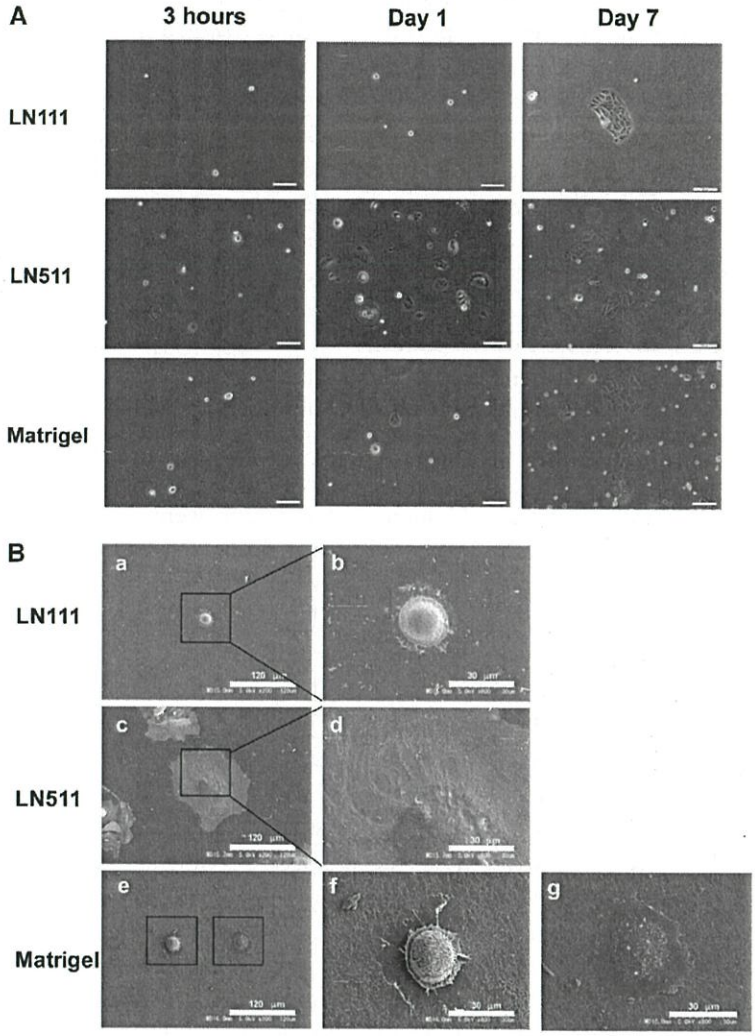

FIG. 1. Phase-contrast and scanning electron microscopy images of second-passage cells cultured on Matrigel-coated, LN111-coated, or LN511 (E8 fragment)-coated plates. The SHs sorted by anti-CD44 Ab were cultured on Matrigel-coated dishes for 28 days. (A) The first-passage cells were trypsinized and plated on Matrigel-coated, LN111-coated, or LN511-coated 35-mm dishes. Photos were taken at 3 hours, 1 day (day 1), and 7 days (day 7) after plating. Scale bars: 200 μm. (B) Images of the second-passage cells attached to LN111 (a,b), LN511 (c,d), or Matrigel (e-g) at day 1 were obtained by scanning electron microscopy. Enlarged versions of the boxed regions of the cells on LN111 (a), LN511 (c), and Matrigel (e) are shown in (b), (d), (f), and (g), respectively. Scale bars: 120 μm (a,c,e) and 30 μm (b,d,f,g).

LN521 showed features similar to those on LN511 (Supporting Fig. S2A). Colonies with different shapes were formed on Matrigel at day 7 and later: One was a colony in which small cells compactly gathered, and the other featured cells with a large cytoplasm loosely contacting each other. The former was often found on LN111, whereas the latter was only on LN511. These results indicate that the typical features of colonies consisting of HPPCs (i.e., small, polygonal-shaped cells) occurred on LN111 and Matrigel that contained LN111. This suggested that interactions between cells with LN111 but not with LN511 may contribute to maintaining the characteristics of HPPCs. Because the behavior of cells on LN521 was similar to that on LN511, subsequent experiments were performed using LN511-coated culture devices.

To examine whether the first-passage cells consisted of different types of cells exhibiting distinct abilities

to bind to different LN isoforms, we collected the cells that did not attach to LN111-coated dishes and transferred them to LN511-coated ones (Supporting Fig. S3A). Three hours after plating cells onto LN111-coated dishes, the medium containing unattached cells was collected and poured into LN511-coated dishes. One hour after plating, many cells had attached and exhibited a flattened shape on the LN511-coated dishes, whereas the cells attached to the LN111-coated ones still maintained spherical features even though 4 hours had passed since plating (Supporting Fig. S3B). Four hours after separation, the cells on dishes coated with each ECM were harvested. Their gene expression was comprehensively analyzed using oligo microarrays. Cells were also cultured for 7 days before assessing the efficiency of colony formation by counting the numbers of cells in images taken 7 days after plating. Colonies typical of HPPCs were formed in the LN111-coated and Matrigel-coated dishes, but not in the LN511-coated ones (Supporting Fig. S3B). Colony sizes and the number of cells forming the colonies were quantified and are given in Supporting Table S3. The largest number of cells per colony was observed in the dishes coated with LN111. The average sizes of the cells on LN111 were significantly smaller than those on LN511, although the labeling index on day 7 did not differ among the three ECMs. Furthermore, the cells cultured on LN111 retained the ability to form HPPC colonies after passaging (Supporting Fig. S4A). The level of albumin (*Alb*) and *Cd44* expression was maintained in the cells cultured on LN111, even after four passages (Supporting Fig. S4B). However, when cells cultured on LN511 were separated and replated onto LN111- and Matrigel-coated dishes, they could not form HPPC colonies in any dishes.

Figure 2 shows heat maps of selected genes related to hepatic function and hepatic stem cells that were expressed in the cells 4 hours after passage. The expression of genes related to hepatic function in the cells on Matrigel showed a tendency to be higher than in the cells on both LN111 and LN511, although the absolute values in the cells on Matrigel were much lower than those in MHs. Representative gene expression (*Alb*, hepatocyte nuclear factor 4α [*Hnf4α*], and CCAAT/enhancer binding protein α [*C/ebpα*]) was confirmed using qRT-PCR (Fig. 2C). The expression of such genes in the cells on Matrigel, LN111, and LN511 was much lower than that in MHs, although the expression of *Hnf4α* in the cells on Matrigel was as high as that in MHs. *Afp* was expressed in the passaged cells (Supporting Fig. S5). Genes related to cholangiocytes, such as *Krt19*, *Sox9*, and *EpCAM*, were more expressed in cells grown on LN511 than on LN111, whereas the expression of genes related to hepatic stem cells, such as *Thy1*, *c-Kit*, and *CD24*, appeared not to differ between the cells grown on LN111 and on LN511. The fact that the gene expression pattern clearly differed between the cells grown on LN111 and on LN511 may indicate that the colonies formed during culturing of the first-passage cells consisted of two distinct populations.

The separate populations also expressed distinct integrins (Fig. 3A). The gene-expression pattern of integrin subunits (α-chains and β-chains) differed between cells grown on LN111 and LN511. The cells grown on LN111 were close to those grown on Matrigel. These microarray results were confirmed by qRT-PCR (Fig. 3B). Integrin β1 was expressed in all cells. Integrins α1, α5, αv, and β3 were highly expressed in cells grown on LN111, whereas α3, α6, and β4 were highly expressed in cells grown on LN511, of which integrins α3, α6, α7, β1, and β4 are known as those of the LN receptor.[12] The cells grown on Matrigel and primary $CD44^+$ cells expressed the genes by cells grown on both LN111 and LN511. The gene expression of integrin α3, α6, α7, β1, and β4 was confirmed using qRT-PCR (Fig. 3C). Both α6 and β4 genes were expressed more in the cells grown on LN511 than in those grown on LN111, whereas the β1 gene was significantly more highly expressed in the cells grown on LN111 than in the cells on LN511. The expression of the α7 gene was extremely low in all cells examined. To investigate the production of the proteins encoded by these proteins, we performed double immunocytochemistry for the integrins α6β1/β4 and integrin α3/HNF4α in the colonies (Fig. 4A). HPPCs in dishes coated with LN111 and Matrigel were positive for integrin α6β1 and integrin α3 and weak or negative for integrin β4 (Fig. 4). However, anti-integrin β4 was stained in the cytoplasm of relatively large cells observed in dishes coated with LN511. These results indicate the discrepancy between gene and protein expression in hepatocytic progenitor cells and that the expression pattern of integrins differed between hepatocytic progenitor cells on LN111 and LN511.

It has been reported that pluripotent stem cell (PSC)-derived hepatoblast-like cells maintain their ability to self-renew when grown on LN111 through integrin α6β1.[15] In this study, small-sized cells

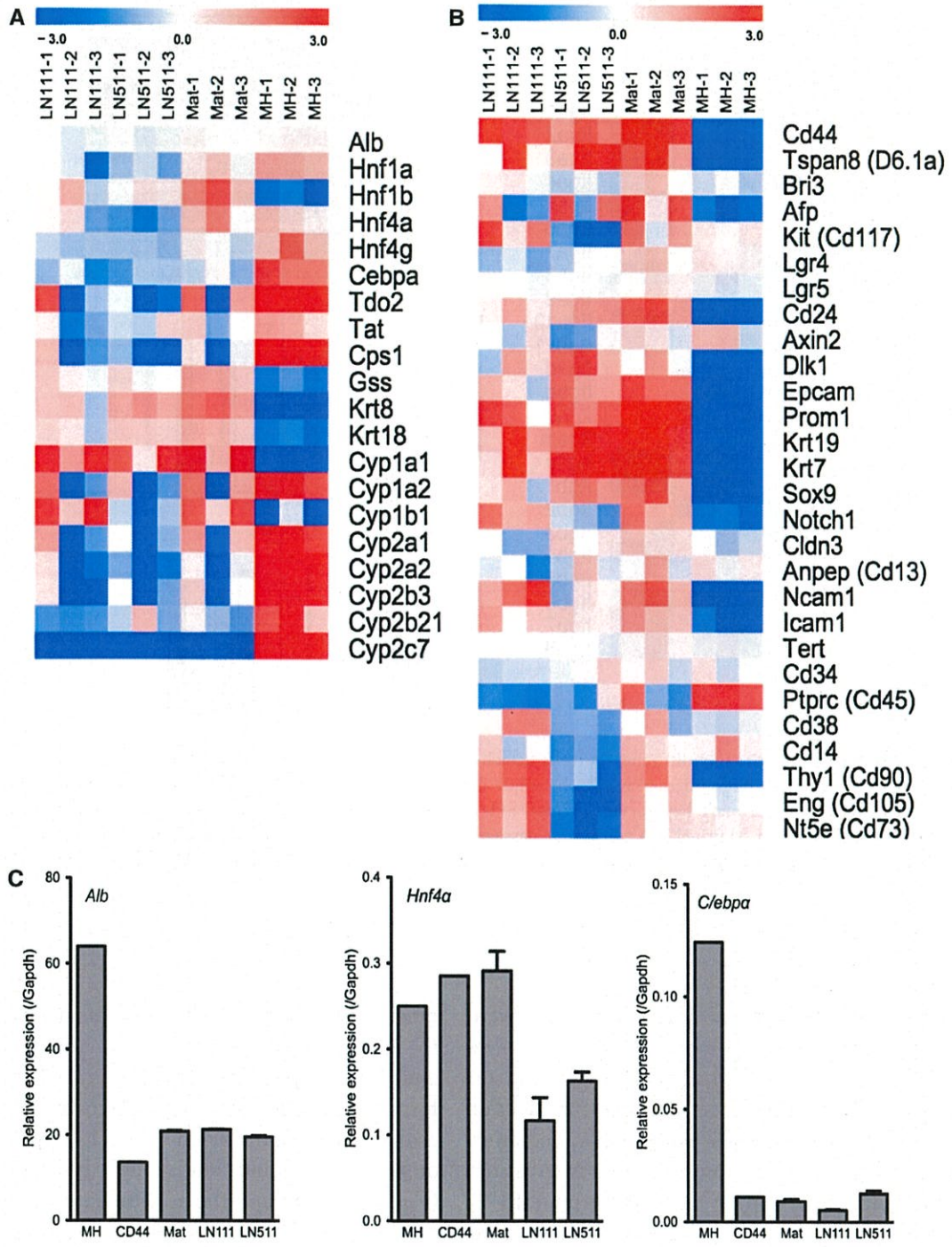

FIG. 2. Comprehensive analysis of gene expression of second-passage cells attached to L111, LN511 (E8 fragment), or Matrigel. The relative expression of selected genes related to hepatic function (A) and stem cell markers (B) was analyzed using oligo microarrays. The first-passage cells cultured on Matrigel for 28 days were trypsinized and plated on LN111-coated dishes (Supporting Fig. S3A). Unattached cells in the medium were collected and replated on LN511-coated dishes. The cells were harvested 4 hours after passage. Primary hepatocytes (MH-1-3) were used as a control. (C) Differences in gene expression related to hepatic function between the cells attached on L111, LN511, and Matrigel were analyzed by qRT-PCR. MHs were used as a reference. Bars depict means ± SEM of three dishes. Abbreviations: GAPDH, glyceraldehyde 3-phosphate dehydrogenase; Mat, Matrigel.

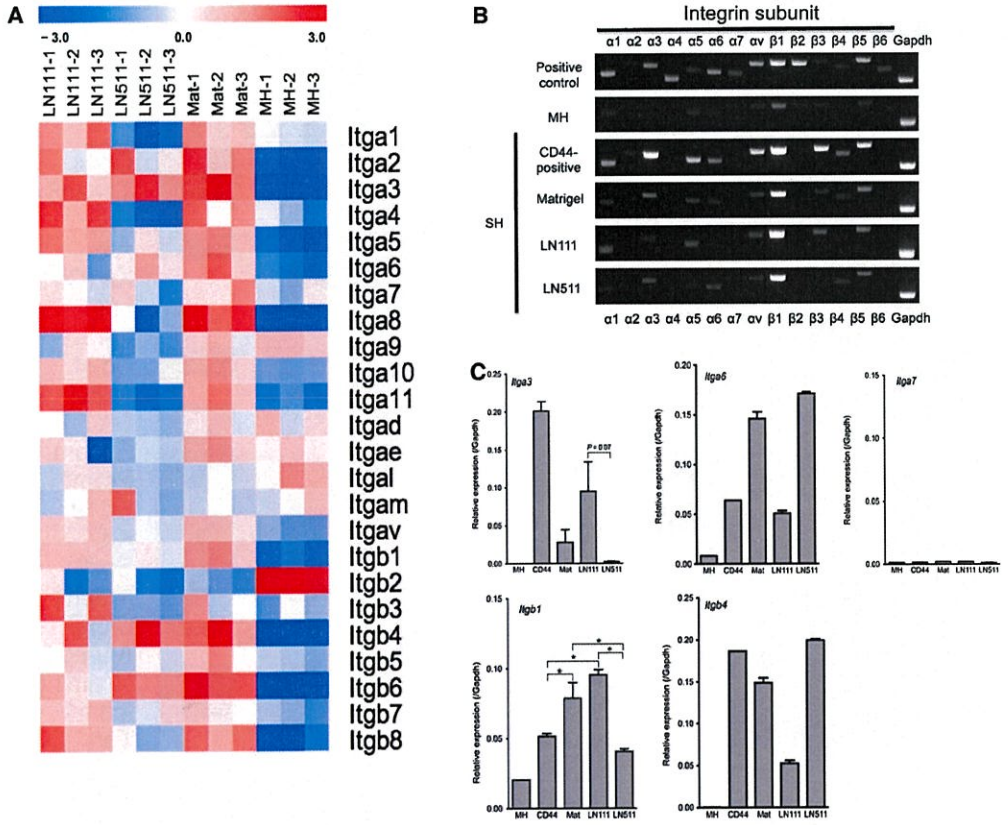

FIG. 3. Expression of integrin subunit genes by cells attached to L111, LN511(E8 fragment),or Matrigel. (A) Comprehensive expression was analyzed using oligo microarrays. Each sample is the same as used for Fig. 2. (B) Expression of integrin subunit genes was analyzed by qRT-PCR; primary hepatocytes (MHs), SHs sorted by anti-CD44-Ab (CD44-positive), and second-passage cells attached to LN111, LN511, or Matrigel at 4 hours after passage. (C) Specific integrin subunits (α3, α6, α7, β1, and β4) were analyzed by qRT-PCR. The bars represent the means ± SEM of the three dishes. $^*P < 0.05$. Abbreviation: GAPDH, glyceraldehyde 3-phosphate dehydrogenase.

comprising the colonies on Matrigel/LN111 were positive for integrins α6β1 and α3. Therefore, we used FACS to analyze integrin α6β1 expression on first-passage cells that had been cultured for 21 days. We found that integrin α6β1 expression varied from low to high (Fig. 5A). Therefore, we sorted two distinct populations, integrin $\alpha6\beta1^{high}$ and integrin $\alpha6\beta1^{low}$, plated them onto LN111-coated and LN511-coated wells, and cultured them for 28 days. Approximately 30% of plated integrin $\alpha6\beta1^{high}$ cells attached to the LN111-coated wells, whereas only approximately 3% of integrin $\alpha6\beta1^{low}$ cells did the same (Fig. 5B). The attachment ratio of integrin $\alpha6\beta1^{high}$ and integrin $\alpha6\beta1^{low}$ cells to LN511-coated wells was approximately 45% and 15%, respectively. The attachment rates of integrin $\alpha6\beta1^{high}$ and integrin $\alpha6\beta1^{low}$ cells to Matrigel-coated ones were approximately 40% and 10%, respectively. Integrin $\alpha6\beta1^{high}$ cells could form typical colonies in LN111-coated and Matrigel-coated wells but not in LN511, whereas integrin $\alpha6\beta1^{low}$ cells could not in any ECM-coated wells (Fig. 5C). Although the attachment rate of the sorted cells was much higher to LN511-coated wells than to LN111-coated ones, colonies typical of HPPCs developed only in LN111-coated and Matrigel-coated wells, not in the LN511-coated ones. The fate of integrin $\alpha6\beta1^{high}$ cells on LN111 versus LN511 suggests that HPPCs may alter their cellular features and lose their ability to self-renew on LN511. Integrin α3 was also expressed more highly in the cells on LN111 than

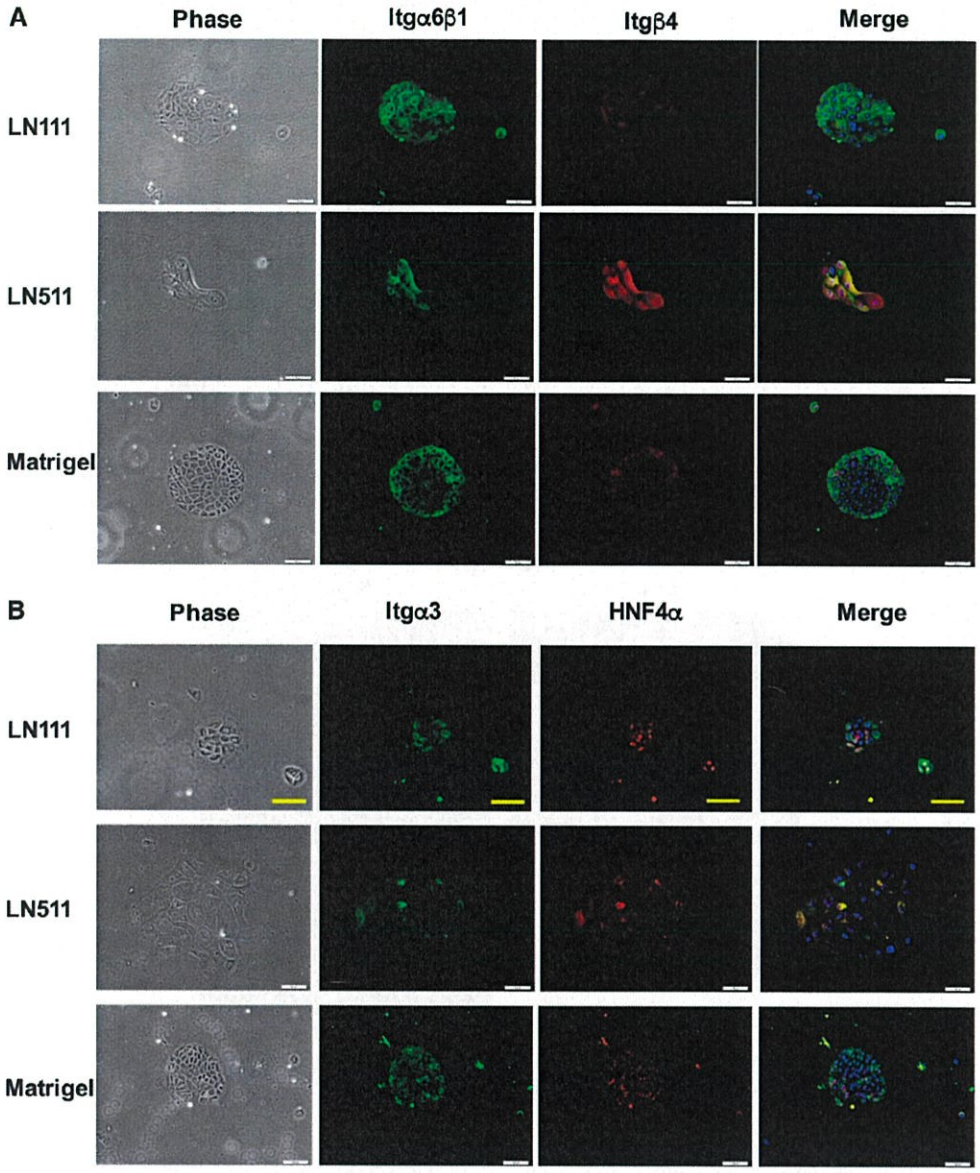

FIG. 4. Fluorescent immunocytochemistry for integrins in second-passage cells on LN111, LN511 (E8 fragment), or Matrigel. Photos of fluorescent immunocytochemistry for integrin α6β1 and integrin β4 (A), and integrin α3 and HNF4α (B), are shown for the second-passage cells cultured on LN111, LN511, and Matrigel for 2 weeks. 4′,6-diamidino-2-phenylindole was used as a nuclear marker. Scale bars: 100 μm.

those on LN511 (Fig. 3C). Therefore, first-passage cells were sorted by the expression of integrins α6β1 and α3 (Fig. 6A). The sorted cells were divided into three subpopulations: integrin (Itg) $\alpha3^{high}\alpha6\beta1^{high}$ (30%), Itg $\alpha3^{low}\alpha6\beta1^{high}$ (34%), and Itg $\alpha3^{low}\alpha6\beta1^{low}$ (36%). The attachment rates of Itg $\alpha3^{high}\alpha6\beta1^{high}$, Itg $\alpha3^{low}\alpha6\beta1^{high}$, and Itg $\alpha3^{low}\alpha6\beta1^{low}$ cells on LN111 were approximately 5%, 1.5%, and 1%, respectively (Fig. 6B). Only integrin $\alpha3^{high}\alpha6\beta1^{high}$ cells could form HPPC colonies in the LN111-coated wells (Fig. 6C), whereas integrin α3-negative ones could not. These results suggest that HPPCs express integrin $\alpha3^{high}\alpha6\beta1^{high}$.

Because the integrin β-chain plays an important role in signal transduction, an integrin β1-neutralizing antibody (Ab) was used to determine

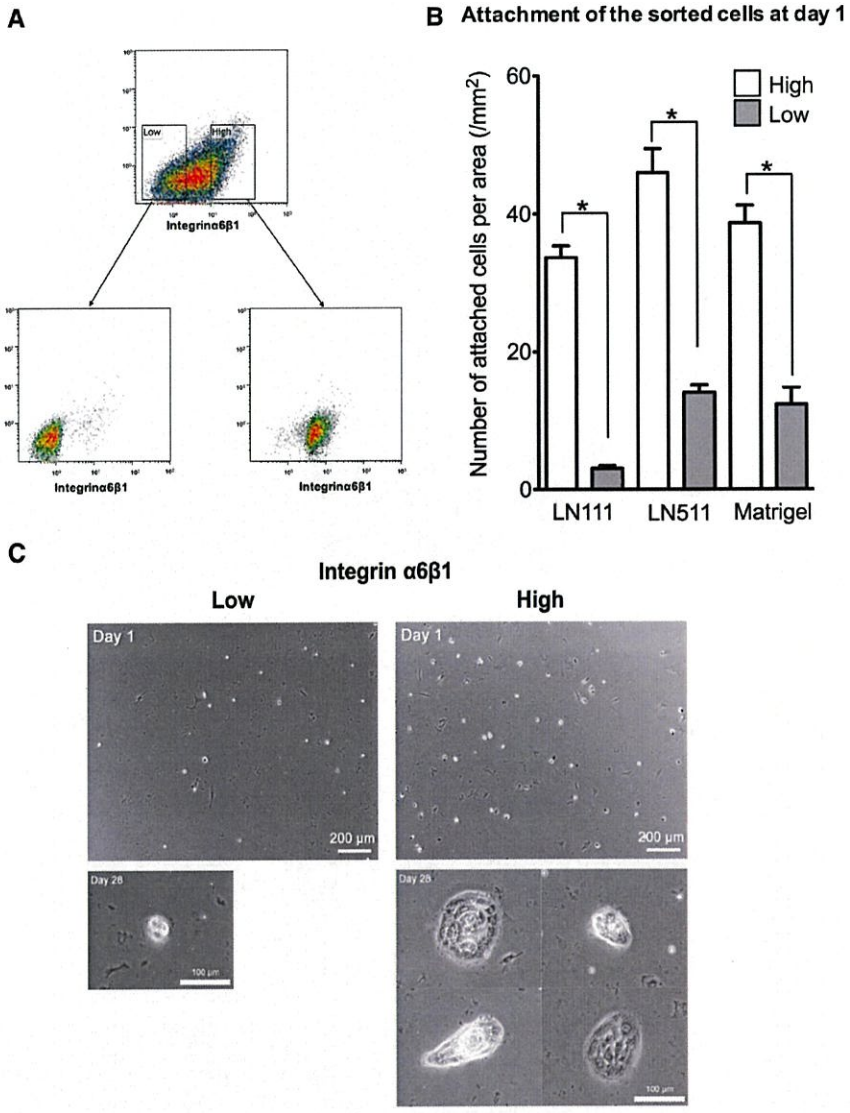

FIG. 5. Attachment and growth of the cells sorted by anti-integrin α6β1 antibody. (A) Cells isolated from first-passage cells were cultured on Matrigel for 28 days and sorted by FACS. Expression of integrin α6β1 varied from low to high. Two distinct populations, integrin $\alpha6\beta1^{high}$ and integrin $\alpha6\beta1^{low}$ cells, were sorted. The sorted cells were plated on LN111-coated, LN511(E8 fragment)-coated, and Matrigel-coated wells of 12-well plates and cultured for 28 days. (B) The number of attached cells was counted 1 day after plating. Bars represent the means ± SEM of three wells. The data were analyzed by ANOVA with Tukey's multiple comparison test. $^*P < 0.05$. (C) Phase-contrast images of sorted cells were taken, and colonies were observed on day 28. Integrin $\alpha6\beta1^{low}$ cells rarely formed a colony, and typical colonies observed at 28 days after plating are shown. Scale bar: 200 μm (day 1), 100 μm (day 28).

whether the Ab inhibits colony formation by HPPCs. Although the Ab remarkably suppressed the attachment of cells to LN111, it did not inhibit attachment to LN511 (Fig. 7A). The initial 48 hours of treatment by the Ab was also enough to inhibit HPPCs from forming colonies on LN111 and Matrigel, and the number of colonies decreased 7 days after plating (Fig. 7B). In contrast, $CD44^+$ HPPC colonies were not formed on LN511 in the presence or absence of neutralizing Ab. Next, we investigated whether HPPC colony formation depended on a signal from LN111; therefore, an inhibition assay using anti-LN111 Ab was conducted (Fig. 7C). The attachment of cells plated onto LN111 and Matrigel

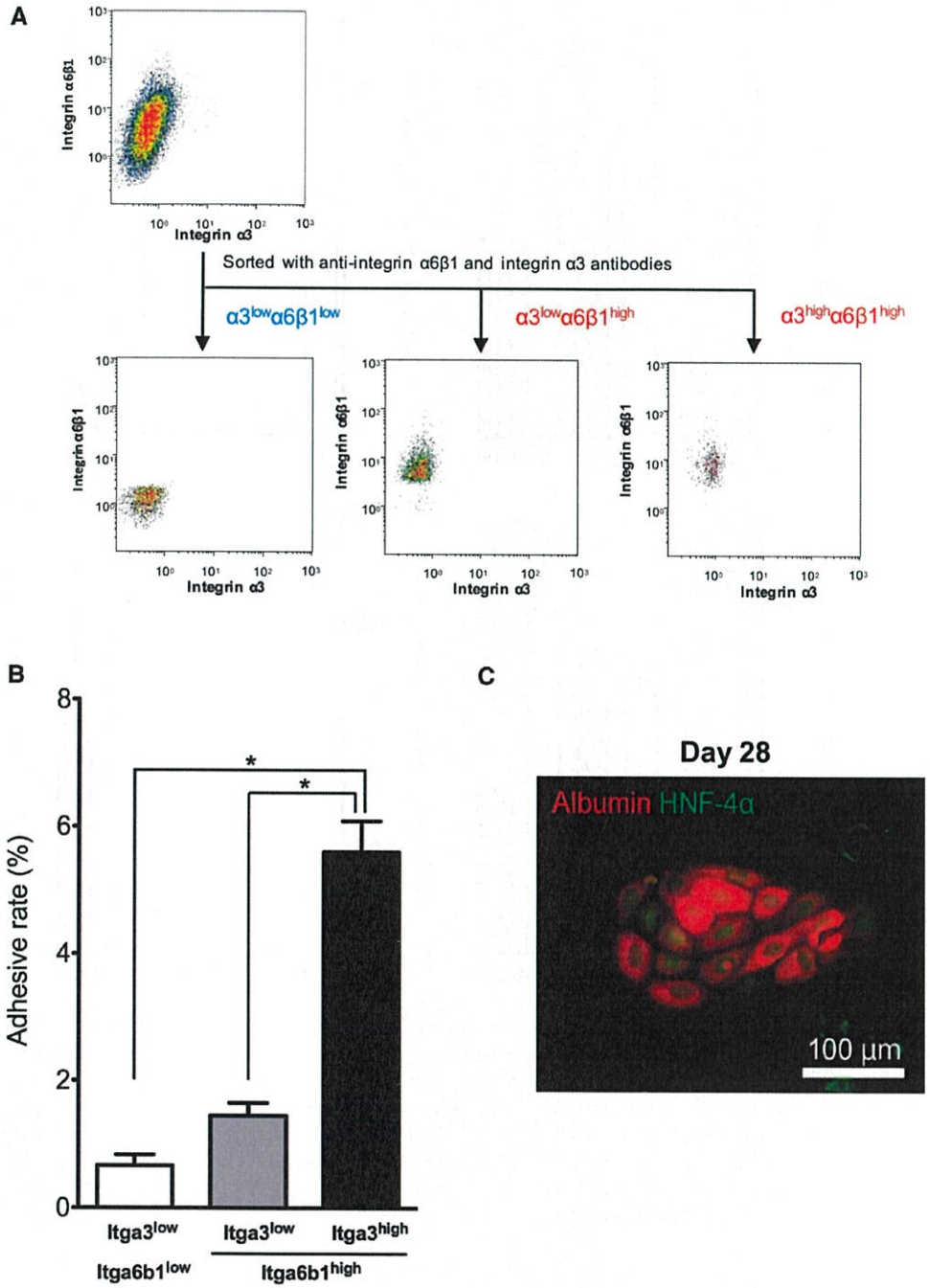

FIG. 6. Attachment and growth of the cells sorted by anti-integrin α3 and integrin α6β1 antibodies. (A) Cells isolated from first-passage cells were cultured on Matrigel for 28 days and sorted by FACS. Expression of integrin α3 varied from low to high in $\alpha6\beta1^{high}$ cells. The integrin-$\alpha6\beta1^{low}/\alpha3^{low}$, $\alpha6\beta1^{high}/\alpha3^{low}$, and $\alpha6\beta1^{high}/\alpha3^{high}$ cells were sorted. The sorted cells were plated on LN111-coated wells of 12-well plates and cultured for 28 days. (B) The number of attached cells was counted 1 day after plating. The data were analyzed by ANOVA with Tukey's multiple comparison test. Bars represent the means ± SEM of three wells. $^*P < 0.05$. (C) Immunocytochemistry for albumin/HNF4α was performed in the colony formed by sorted $\alpha6\beta1^{high}/\alpha3^{high}$ cells that were cultured on LN111 for 28 days. Scale bar: 100 μm (day 28).

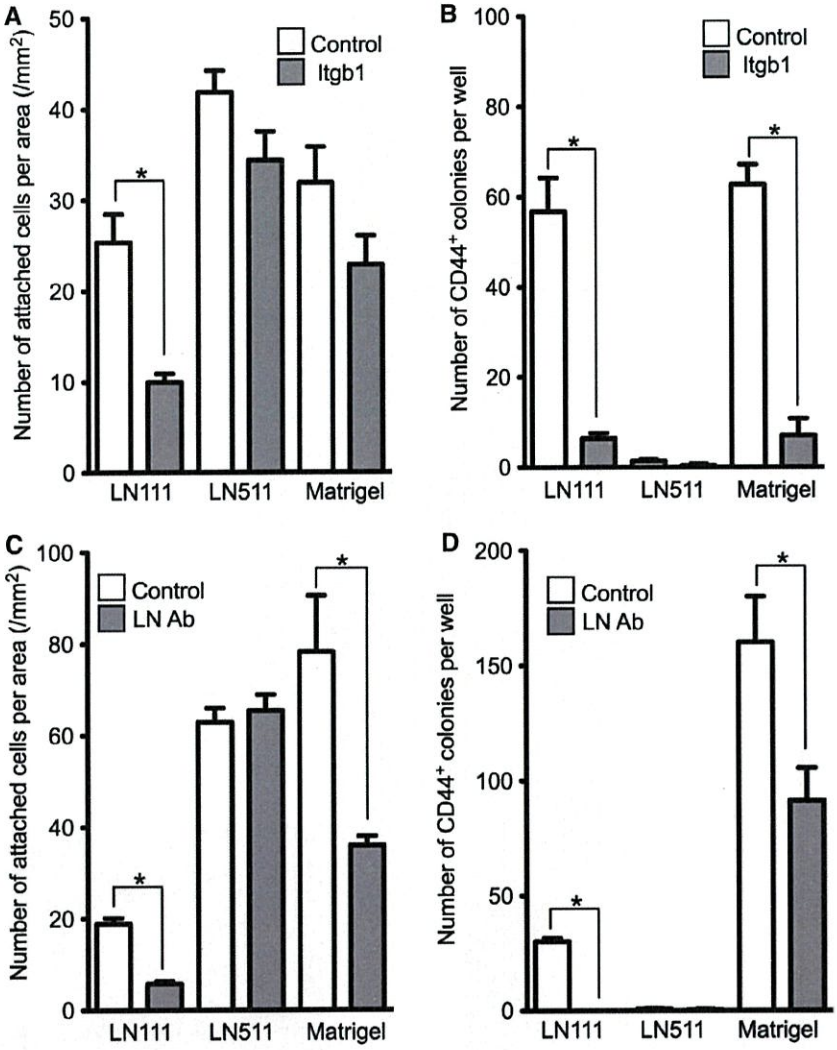

FIG. 7. Integrin β1 and LN111 dependence of cell attachment and colony formation. First-passage cells cultured on Matrigel for 28 days were collected by trypsinization. The isolated cells were incubated for 2 hours in the medium containing antirat integrin β1 hamster immunoglobulin M antibody or hamster immunoglobulin M isotype standard. The cells were plated on LN111-coated or LN511 (E8 fragment)-coated 12-well plates. The rates of cell attachment (A) and colony formation (B) were assessed at day 1 and day 7, respectively. In the same way, the isolated cells were plated on LN111-coated, LN511-coated, or Matrigel-coated 12-well plates and cultured in the medium containing rabbit anti-LN111 or goat antirabbit immunoglobulin G antibody. The rates of cell attachment (C) and colony formation (D) were assessed at day 1 and day 7, respectively. All data were analyzed using ANOVA with Tukey's multiple comparison test. $^*P < 0.05$. Bars represent the mean ± SEM of three wells.

in the presence of anti-LN111 Ab was significantly inhibited, whereas that of the cells similarly plated onto LN511 was not. HPPC colony formation on LN111 and Matrigel was also clearly suppressed by the neutralizing Ab (Fig. 7D). This result demonstrates that a signal from LN111 is crucial for HPPCs' growth.

HPPCs attached to both LN111 and Matrigel generated a different type of colony as well as HPPCs, the features of which were similar to those of the colonies observed on LN511 (Fig. 1A). Because LNα5 was initially not present in either the LN111-coated or the Matrigel-coated dishes, we examined the production of LN subunits in cells attached to L111-, LN511-,

and Matrigel-coated dishes. No cells expressed LNα1 (Supporting Fig. S6A). However, with the exception of MHs, the cells could produce the LNα5-chain. Comprehensive analysis of ECMs produced by cells (Supporting Fig. S6B) illustrated that, in addition to many kinds of ECM-related genes, including those encoding many more isoforms of collagens, nidogens, and tenascin than those attached to LN511, cells attached to both Matrigel and LN111 expressed LNα5, β1, and γ1, suggesting that they produce LN511. These results indicate that the LN511 produced by HPPCs on Matrigel and LN111 may support the survival and proliferation of their daughter cells that are typically found on LN511.

We then examined whether inducing maturation differed between cells on LN111 and those on LN511 by overlaying cell cultures for 7 days with Matrigel. Cells without MGOL (control) retained flat-shaped colonies (Fig. 8A). As a result, cells on both Matrigel and LN111 formed 3D structures, whereas colonies on LN511 shrank (Fig. 8A). When FD was added to the culture medium, cells retained fluorescence in their cytoplasm in the colonies without MGOL, because BC between the cells were not well assembled. However, in colonies formed on both Matrigel and LN111, fluorescence was secreted into BC, illustrating the presence of well-developed BC networks. After MGOL, cell colonies on LN111 and Matrigel increased the expression of genes related to hepatic functions, such as *Alb*, *Tat*, *Tdo2*, and *Cyp1a2* (Fig. 8B). *Alb* and *Tat* expression, in particular, increased significantly in cells on both LN111 and Matrigel, and *Tdo2* expression increased significantly in cells on Matrigel. In contrast, MGOL did not induce hepatic differentiation in cells on LN511. Because *Cd44* and *Krt19* expression was significantly suppressed in cells on both LN511 and Matrigel, inefficient induction of hepatocyte differentiation was not caused by maintaining an immature state or committing to the cholangiocyte lineage (Supporting Fig. S7).

Discussion

Our previous study revealed that HPPCs are present among CD44$^+$ SHs.[10] These cells retain their capability to proliferate and redifferentiate but gradually lose their ability to self-renew. Furthermore, we found that two types of morphologically distinguishable colonies emerged during the culture of HPPCs: One type is round and consists of homogeneously small-sized mononuclear cells, and the other consists of cells with large cytoplasm. Therefore, we speculated that the small cells forming round colonies were HPPCs, whereas the other large cells were daughter cells derived from HPPCs. In the present study, we clarified the mechanism behind the maintenance of self-renewal of HPPCs, to analyze their characteristics and those of their daughter cells.

We have reported that HPPCs can be passaged only in dishes coated with Matrigel.[10] In addition, fewer than 20% of passaged cells could attach to Matrigel-coated dishes. When passaged cells were plated on a dish coated with LN111, their attachment rate was slightly lower than those on Matrigel. Whenever colonies grown on LN111 were passaged, less than 20% of the cells could attach, and this rate gradually decreased with increasing passages. These results suggest that the number of HPPCs decreases with increasing passages. In addition, many cells derived from HPPCs can attach not to LN111 but to LN511. In fact, when first-passage cells are separated and plated on LN111, the unattached cells can still attach to LN511. Furthermore, HPPCs possessing the ability to self-renew have never emerged on LN511. These results also suggest that HPPCs generate two distinctive cell populations and that many HPPCs perform asymmetric cell division. One division is LNα1-dependent, and the other is LNα5-dependent. In addition, the fact that LN111-neutralizing Ab suppresses colony formation of HPPCs on LN111 also supports the idea that HPPCs' self-renewability is LN111-dependent. The survival and proliferation of LNα5-dependent daughter cells may be supported by LNα5 produced by passaged cells.

Maintenance of the ability of stem cells to self-renew on LN111 has been reported in hepatoblast-like cells derived from human-induced PSCs (HiPSCs).[15] Undifferentiated HiPSCs can be maintained on LN511 but not on LN111.[16] These results suggest that LN111 could not only selectively maintain hepatoblast-like cells but also eliminate residual undifferentiated cells. It has been reported that, in human liver development, LN is present in both the perisinusoidal space and portal tract.[17] In fetal mouse liver, LNsα1 and α5 have been detected at the basal side of cholangiocytes, whereas only LNα5 was detected in the adult liver.[18] Interestingly, EpCAM$^+$

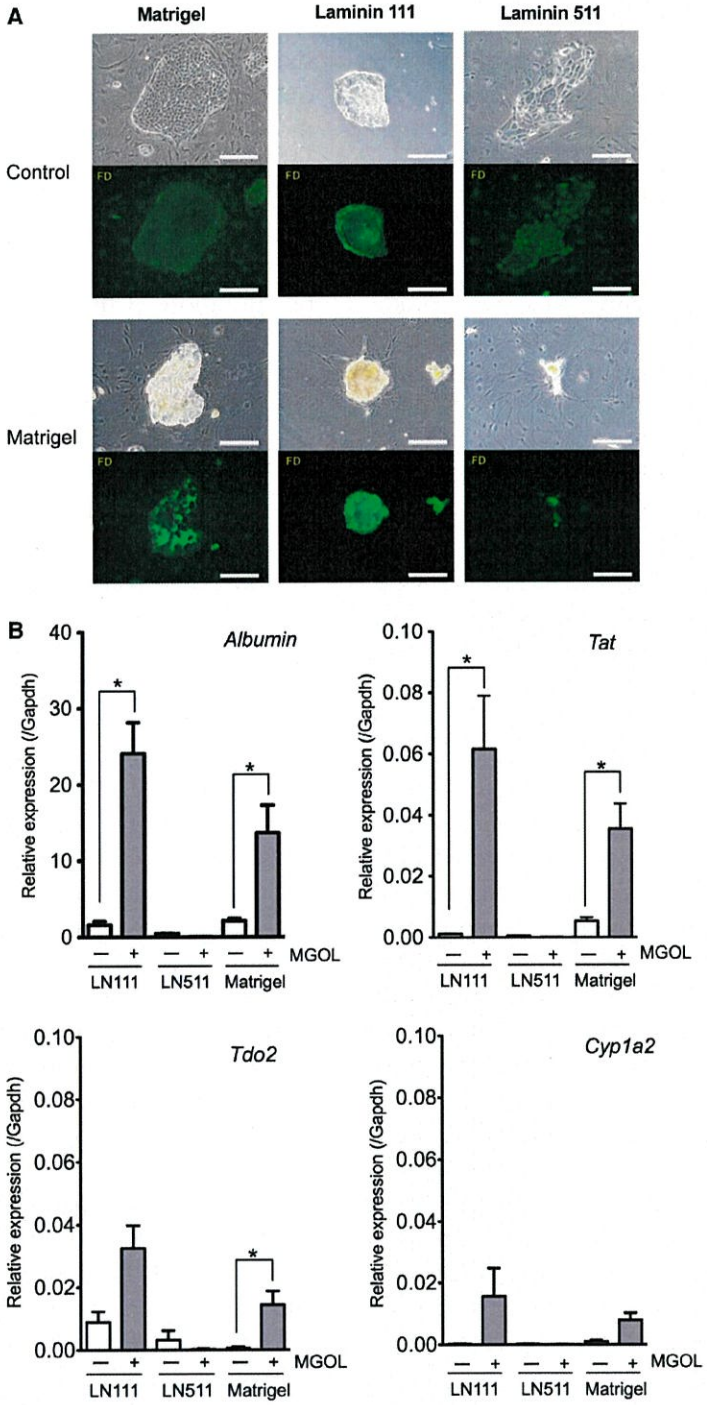

FIG. 8. Maturation of colonies of second-passage cells on each ECM after MGOL. The second-passage cells were cultured on Matrigel-coated, LN111-coated, or LN511 (E8 fragment)-coated dishes for 14 days and treated with medium containing or lacking (control) 5% Matrigel for 7 days. (A) To examine the formation of BC, the cells were incubated with FD. After incubation with FD, the phase contrast and fluorescent images were obtained. BC were formed after MGOL by the colonies of cells cultured on Matrigel or LN111. No colonies without MGOL formed BC. Scale bars: 200 μm. (B) Gene expression related to hepatic function in the cells, with or without MGOL, was analyzed by qRT-PCR. All data were analyzed using Kruskul–Wallis ANOVA with Dunn's multiple comparison test. $^{*}P < 0.05$). Bars represent the mean ± SEM of three dishes.

cells are bipotential during both the fetal and neonatal stages but later lose this ability. It is possible that EpCAM$^+$ cells can keep their bipotency only in the presence of LN111. On the other hand, hepatoblasts isolated from mouse E14 fetal liver kept their bipotency when grown on LN111.[19] Intercellular cell adhesion molecule-1 (ICAM-1)$^+$ liver progenitor cells separated from late-fetal and postnatal mouse livers could also maintain their ability to self-renew on LN111 after passages.[20] Thus, hepatic cells with fetal characteristics or less differentiated hepatocytes may acquire the ability to proliferate in an LNα1-dependent manner.

In liver regeneration after partial hepatectomy, studies have indicated that regeneration may be achieved by the simple duplication of MHs, and hepatic stem/progenitor cells do not contribute to this type of liver regeneration.[21-25] However, recent studies have revealed that MHs maintain the potential to dedifferentiate into immature hepatocytes and transdifferentiate into cholangiocytes, suggesting that they possess plasticity.[26-29] More recently, Axin2$^+$ pericentral hepatocytes were reported to be the physiological progenitors of hepatocytes during cellular turnover in normal mouse liver[26]; however, there is still controversy about this.[27] Conversely, we have reported that Sox9$^+$EpCAM$^-$ biphenotypic hepatocytes derived from MHs emerge adjacent to expanding ductal structures in 3,5-diethoxycarbonyl-1,4-dihydrocollidine-fed mouse livers.[28] Sox9$^+$ periportal hepatocytes have also been identified as hepatocyte progenitors during regeneration from chronic liver injury. Furthermore, we have shown that small, mononuclear hepatocyte progenitors are present in ICAM-1$^+$ fractions.[20] The ICAM-1$^+$HNF4α$^+$ mononuclear cells, isolated from healthy adult mouse livers, did not specifically localize to liver lobules and exhibited low expression of both *Axin2* and *Lgr5* genes. On the other hand, HPPCs express *Lgr5*, whereas their *Axin2* gene expression is much lower than that of MHs. These accumulated findings suggest that MHs contain a subpopulation of cells possessing the potential to become self-renewable progenitor cells with the ability to redifferentiate. Whether or not a single subpopulation of MHs possesses progenitor potential, and where these cells localize to in a liver lobule, remains to be determined.

It is important to elucidate the differences between ECM-based ligands and their receptors in HPPCs and their progeny. Although the progeny proliferating on LN511 can still grow while retaining hepatocytic characteristics, this potential varies among cells and is lower than in HPPCs. It is known that LN511, LN332, and LN111 share a high affinity for integrin α6β1.[16,30] Using function-blocking Abs, integrin α6β1 has been identified as the major cell adhesion receptor for cells on both Matrigel and LN111. It is also known that integrin α6β1 is abundantly expressed by PSCs[31] and hepatoblast-like cells derived from PSCs.[15] On the other hand, integrin α6β1$^+$ cells isolated from fetal mouse livers have been shown to form colonies consisting of cells expressing both hepatocyte and biliary markers.[32] Of those cells, c-Met$^+$CD49f (integrin α6)$^{+/low}$ c-Kit$^-$ cells were the most potent with respect to self-renewal and differentiation.[33]

Tissue homeostasis in skeletal muscles relies on the activities of muscle-specific stem cells, called satellite cells (SCs).[34] When SCs are activated, a remodeling event, mediated by matrix metalloproteinases, leads to the deposition of LNα1 and LNα5 at the SC niche during muscle regeneration.[35] Loss of LNα1 function impairs SC proliferation and self-renewal, resulting in decreased long-term regenerative ability. LN111 mediates its effect through integrin-α6β1 signaling. The LN111/integrin-α6β1 axis has been associated with the long-term self-renewal of hepatoblast-like cells derived from HiPSCs,[15] with the sphere-forming capacity of human prostate cancer stem cells and neural stem cells[36,37] and with asymmetric cell division of *Drosophila* ovarian follicle stem cells.[38] Therefore, it is likely that the interaction between LN111 and integrin-α6β1 represents an ancient mechanism to maintain stem cell self-renewal.[35] In this study, only integrin-α3^{high}α6β1^{high} cells could form HPPC colonies, and both anti-integrin β1 and anti-LN111-neutralizing Ab suppressed the attachment of, and colony formation by, these HPPCs. Thus, HPPCs' self-renewal capabilities depend on LN111 by integrin β1 signaling.

While Matrigel-containing LN111 plays an essential role in the expansion of HPPCs, it also induces hepatocytic maturation, which is accompanied by hepatic organoid formation. This phenomenon was also supported by the results from differentiation-related gene expression. Considering that the administration of a single component of Matrigel, such as LN111, type IV collagen, or nidogen, did not induce 3D structural change of a colony by HPPCs (data not

shown), the 3D structure of a combination of some constituents present in Matrigel may be important for inducing the conformational changes of HPPCs, which results in hepatocytic maturation.

In the present study, we have shown that HPPCs' self-renewal capability depends on LN-α1 and that the signal is transmitted through integrin β1, and HPPCs can easily expand on LN111-coated culture devices in serum-free medium. Although some improvements to the procedure may be required to isolate human HPPCs, this method might generate large numbers of healthy hepatocytes from a limited number of donors or surgically resected liver.

Acknowledgment: We thank Ms. Yumiko Tsukamoto and Ms. Minako Kuwano for their technical assistance, Dr. Yamato Kikkawa (Tokyo University of Pharmacy and Life Sciences) and Prof. Kiyotoshi Sekiguchi (Osaka University) for their valuable advice, and Enago (www.enago.jp) for the English language review.

REFERENCES

1) Fisher RA, Strom SC. Human hepatocyte transplantation: worldwide results. Transplantation 2006;82:441-449.
2) Yarygin KN, Lupatov AY, Kholodenko IV. Cell-based therapies of liver diseases: age-related challenges. Clin Interv Aging 2015;10:1909-1924.
3) Bhatia SN, Underhill GH, Zaret KS, Fox IJ. Cell and tissue engineering for liver disease. Sci Transl Med 2015;6:245sr2.
4) Mitaka T. The current status of primary hepatocyte culture. Int J Exp Pathol 1998;79:393-409.
5) Mitaka T, Ooe H. Drug metabolism reviews focusing on drug transporter interactions in the liver: characterization of hepatic-organoid cultures. Drug Metab Rev 2010;42:472-481.
6) Mitaka T, Norioka K, Sattler GL, Pitot HC, Mochizuki Y. Effect of age on the formation of small-cell colonies in cultures of primary rat hepatocytes. Cancer Res 1993;53:3145-3148.
7) Chen Q, Kon J, Ooe H, Sasaki K, Mitaka T. Selective proliferation of rat hepatocyte progenitor cells in serum-free culture. Nat Protoc 2007;2:1197-1205.
8) Sasaki K, Kon J, Mizuguchi T, Chen Q, Ooe H, Oshima H, et al. Proliferation of hepatocyte progenitor cells isolated from adult human livers in serum-free medium. Cell Transplant 2008;17:1221-1230.
9) Kon J, Ooe H, Oshima H, Kikkawa Y, Mitaka T. Expression of CD44 in rat hepatic progenitor cells. J Hepatol 2006;45:90-98.
10) **Ishii M, Kino J**, Ichinohe N, Tanimizu N, Ninomiya T, Suzuki H, et al. Hepatocytic parental progenitor cells of rat small hepatocytes maintain a self-renewal capability after long-term culture. Sci Rep 2017;7:46177.
11) Kleinman HK, McGarvey ML, Liotta LA, Robey PG, Tryggvason K, Martin GR. Isolation and characterization of type IV procollagen, laminin, and heparan sulfate proteoglycan from the EHS sarcoma. Biochemistry 1982;21:6188-6193.
12) Nishiuchi R, Takagi J, Hayashi M, Ido H, Yagi Y, Sanzen N, et al. Ligand-binding specificities of laminin-binding integrins: a comprehensive survey of laminin-integrin interactions using recombinant α3β1, α6β1, α7β1 and α6β4 integrins. Matrix Biol 2006;25:189-197.
13) Yamada M, Sekiguchi K. Molecular basis of laminin-integrin interactions. Curr Top Membr 2015;76:197-229.
14) Kikkawa Y, Mochizuki Y, Miner JH, Mitaka T. Transient expression of LNα1 chain in regenerating murine liver: restricted localization of laminin chains and nidogen-1. Exp Cell Res 2005;305:99-109.
15) Takayama K, Nagamoto Y, Mimura N, Tashiro K, Sakurai F, Tachibana M, et al. Long-term self-renewal of human ES/iPS-derived hepatoblast-like cells on human LN111-coated dishes. Stem Cell Rep 2013;1:322-335.
16) Rodin S, Domogatskaya A, Ström S, Hansson EM, Chien KR, Inzunza J, et al. Long-term self-renewal of human pluripotent stem cells on human recombinant LN511. Nat Biotechnol 2010;28:611-615.
17) Couvelard A, Bringuier AF, Dauge MC, Nejjari M, Darai E, Benifla JL, et al. Expression of integrins during liver organogenesis in humans. Hepatology 1998;26:839-847.
18) Tanimizu N, Kikkawa Y, Mitaka T, Miyajima A. α1- and α5-containing laminins regulate the development of bile ducts via β1 integrin signals. J Biol Chem 2012;287:28586-28597.
19) Tanimizu N, Miyajima A. Notch signaling controls hepatoblasts differentiation by altering the expression of liver-enriched transcription factors. J Cell Sci 2004;117:3165-3174.
20) Tanimizu N, Ichinohe N, Ishii M, Kino J, Mizuguchi T, Hirata K, et al. Liver progenitors isolated from adult healthy mouse liver efficiently differentiate to functional hepatocytes in vitro and repopulate liver tissue. Stem Cells 2016;34:2889-2901.
21) Forbes SJ, Newsome PN. Liver regeneration–mechanisms and models to clinical application. Nat Rev Gastroenterol Hepatol 2016;13:473-485.
22) Michalopoulos GK. Hepatostat: liver regeneration and normal liver tissue maintenance. Hepatology 2017;65:1384-1392.
23) Miyajima A, Tanaka M, Itoh T. Stem/progenitor cells in liver development, homeostasis, regeneration, and reprogramming. Cell Stem Cell 2014;14:561-574.
24) Merrell AJ, Stanger BZ. Adult cell plasticity in vivo: de-differentiation and transdifferentiation are back in style. Nat Rev Mol Cell Biol 2016;17:413-425.
25) Ober EA, Lemaigre FP. Development of the liver: insights organ and tissue morphogenesis. J Hepatol 2018;68:1049-1062.
26) Wang B, Zhao L, Fish M, Logan CY, Nusse R. Self-renewing diploid Axin2(+) cells fuel homeostatic renewal of the liver. Nature 2015;524:180-185.
27) Planas-Paz L, Orsini V, Boulter L, Calabrese D, Pikiolek M, Nigshe F, et al. The RSPO-LGR4/5-ZNRF3/RNF43 module controls liver zonation and size. Nat Cell Biol 2016;18:467-479.
28) Tanimizu N, Nishikawa Y, Ichinohe N, Akiyama H, Mitaka T. Sry HMG box protein 9-positive (Sox9+) epithelial cell adhesion molecule-negative (EpCAM-) biphenotypic cells derived from hepatocytes are involved in mouse liver regeneration. J Biol Chem 2014;289:7589-7598.
29) Font-Burgada J, Shalapour S, Ramaswamy S, Hsueh B, Rossell D, Umemura A, et al. Hybrid periportal hepatocytes regenerate the injured liver without giving rise to cancer. Cell 2015;162:766-779.
30) Meng Y, Eshghi S, Li YJ, Schmidt R, Schaffer DV, Healy KE. Characterization of integrin engagement during defined human embryonic stem cell culture. FASEB J 2010;24:1056-1065.
31) Miyazaki T, Futaki S, Suemori H, Taniguchi Y, Yamada M, Kawasaki M, et al. Laminin E8 fragments support efficient adhesion and expansion of dissociated human pluripotent stem cells. Nat Commun 2012;3:1236.
32) Suzuki A, Zheng Y, Kondo R, Kusakabe M, Takada Y, Fuka K, et al. Flow-cytometric separation and enrichment of hepatic

progenitor cells in the developing mouse liver. Hepatology 2000; 32:1230-1239.
33) Suzuki A, Zheng YW, Kaneko S, Onodera M, Fukao K, Nakauchi H, et al. Clonal identification and characterization of self-renewing pluripotent stem cells in the developing liver. J Cell Biol 2002;156:173-184.
34) Lepper C, Partridge TA, Fan CM. An absolute requirement for Pax7-positive satellite cells in acute injury-induced skeletal muscle regeneration. Development 2011;138:3639-3646.
35) Rayagiri SS, Ranaldi D, Raven A, Mohamad Azhar N, Lefebvre O, Zammit PS, et al. Basal lamina remodeling at the skeletal muscle stem cell niche mediates stem cell self-renewal. Nat Commun 2018;9:1075.
36) Guo C, Liu H, Zhang BH, Cadaneanu RM, Mayle AM, Garraway IP. Epcam, CD44, and CD49f distinguish sphere-forming human prostate basal cells from a subpopulation with predominant tubule initiation capability. PLoS One 2012;7:e34219.
37) Flanagan LA, Rebaza LM, Derzic S, Schwartz PH, Monuki ES. Regulation of human neural precursor cells by laminin and integrins. J Neurosci Res 2006;83:845-856.
38) O'Reilly AM, Lee HH, Simon MA. Integrins control the positioning and proliferation of follicle stem cells in the Drosophila ovary. J Cell Biol 2008;182:801-815.

Author names in bold designate shared co-first authorship.

Supporting Information

Additional Supporting Information may be found at onlinelibrary.wiley.com/doi/10.1002/hep4.1442/suppinfo.

Supporting Information

Supporting Methods

Laminins used in the experiment

Second-passage cells were plated on 12-well plates coated with laminin (LN)111 (molecular weight [MW] 900 kDa; BD Biosciences, San Jose, CA), LN511-E8 (MW 150 kDa, iMatrix-511; Nippi Inc., Tokyo, Japan), LN511 (MW 800 kDa; BioLamina, Stockholm, Sweden), LN521 (MW 762 kDa; BioLamina), and Matrigel (growth factor-reduced; BD Biosciences). LN511-E8 is a recombinant product of the smallest integrin-binding component. MWs of LN511/LN521 are approximately 5 times that of LN511-E8. Therefore, the concentrations that we used were 11 and 17 μM for LN111 and LN511-E8, respectively.

To examine the concentration dependence of cell attachment on LN111, first-passage cells (75,000 cells/well) were plated on 12-well plates coated with LN111 (Supporting Fig. S1A), and attached cells were counted 1 day after plating. The cells were photographed with a charge-coupled device camera, and the number of cells was counted. LN111 at 10 μg/well was selected for use in the present experiment, and the concentrations of other laminins were adjusted to that of LN111; LN511-E8, LN511, and LN521 were used at 2.5, 10, and 10 μg/well, respectively. Although we also examined the full-length LN511 for the experiment on cell attachment, the adhesion rate of cells did not differ between LN511-E8 and full-length LN511 (Supporting Fig. S1B).

Scanning electron microscopy

The cells were fixed with phosphate-buffered saline (PBS) containing 2.5% glutaraldehyde 24 hours after plating to observe the morphology of cells initially attached to LN111-, LN511-, or Matrigel-coated dishes. After rinsing with PBS, the cells were dehydrated by incubating

through a concentration gradient of ethanol increasing up to 100%. The dehydrated samples were immersed in *t*-butanol and finally dried in a critical point dryer. After sputter coating with gold/palladium, the samples were examined using a scanning electron microscope (S4300; Hitachi, Tokyo, Japan).

Comprehensive gene analysis and polymerase chain reaction

The differences of the expression of genes related to hepatic function and stem cell properties among cells attached to Matrigel, LN111, and LN511 dishes were analyzed with an oligo microarray and quantitative reverse-transcription polymerase chain reaction (qPCR). Four hours after plating on LN111-, LN511-, and Matrigel-coated dishes (Supporting Fig. S3A), the cells were dissolved for total RNA extraction using a TaqMan Gene Expression Cells-to-CT kit (Applied Biosystems, Foster City, CA). Total RNA was extracted from colonies on each extracellular matrix (ECM) and reverse-transcribed using an OmniScript RT kit (Qiagen, Hilden, Germany) and random hexamers. The differences in cell expression profiles were analyzed using an oligo microarray spotted with 30,584 probes (SurePrint G3 Rat Gene Expression v2 G4853B; Agilent Technologies, Santa Clara, CA). All oligo microarray data are registered in the Gene Expression Omnibus (GEO) database (Accession No. GSE126063). The qPCR analyses were completed using TaqMan Gene Expression Assays (Applied Biosystems, Foster City, CA). PCR was performed, in triplicate, for all samples in 96-well optical plates using an ABI Prism 7500 cycler (Applied Biosystems). In addition to the above-mentioned microarray and qPCR analyses, differences in the gene expression of integrin and LN subunit were analyzed by reverse-transcription PCR (RT-PCR). For RT-PCR, complementary DNA (cDNA) was amplified using TaKaRa Ex Taq DNA polymerase (Hot Start Version) with a TaKaRa thermal cycler (Takara Bio Inc., Shiga, Japan). The primers used for (A) qPCR and (B) RT-PCR are listed in Supporting Table S1. *Gapdh* was used to

normalize the relative expression in qPCR and as a control for RT-PCR.

Fluorescent immunocytochemistry

The antibodies used are listed in Supporting Table S2. Cells were fixed in cold absolute ethanol for 15 minutes. After blocking with BlockAce (DS Pharma Biomedical, Osaka, Japan) for 30 minutes at room temperature (RT), the cells were incubated with primary antibody for 60 minutes. The dishes were rinsed with PBS and subsequently incubated with Alexa488- or Alexa594-conjugated secondary antibodies (Molecular Probes) for 30 minutes. Cells were embedded in 90% glycerol containing 0.01% p-phenylenediamine and 4,6-diamidino-2-phenylindole (DAPI).

Measuring the labeling index

Labeling index (LI) was measured by treating cells with 5-bromo-2′-deoxyuridine (BrdU) and subsequently fixing them in cold absolute ethanol for 15 minutes. BrdU was added at 40 μM to the medium 18 hours before fixation. After fixation, the cells were incubated with 2 N HCl for 30 minutes at RT to break DNA double strands. The cells were then incubated with 0.6% hydrogen peroxide in methanol for 30 minutes at RT to eliminate endogenous peroxidase activity. After blocking with BlockAce for 30 minutes at RT, the cells were incubated with primary antibody for 60 minutes. The dishes were rinsed with PBS and subsequently incubated with secondary antibodies (Vector Laboratories, Burlingame, CA) for 30 minutes at RT. Cells were then incubated with avidin-biotin complex solution (VECTASTAIN ABC kit; Vector Laboratories) and treated with 3,3-diaminobenzidine for color development.

Flow cytometry

First-passage cells cultured on Matrigel-coated dishes for 28 days were collected and

incubated with mouse anti-rat integrin α6β1 antibody in Dulbecco's modified Eagle's medium (DMEM)/F12 containing 10% fetal bovine serum (FBS) for 30 minutes at 4°C. Thereafter, cells were washed with PBS containing 2% FBS (Wash Buffer) and centrifuged at 150*g* for 5 minutes. The cells were then incubated with rabbit anti-mouse IgG (H+L) antibody conjugated to Alexa Fluor 488 in DMEM/F12 containing 10% FBS for 30 minutes at 4°C. The cells were then washed with Wash Buffer and centrifuged at 150*g* for 5 minutes. They were next suspended in Wash Buffer containing propidium iodide solution and passed through a 35-μm cell strainer (Corning Inc.). Integrin $\alpha6\beta1^{high}$ or $\alpha6\beta1^{low}$ cells were sorted using a fluorescence-activated cell sorting (FACS) Aria cell sorter (BD Biosciences) and plated on LN111-, LN511, and Matrigel-coated 24-well plates and cultured for 28 days. The medium was replaced 1 day after seeding and then every other day. Data were analyzed using Kaluza Flow Cytometry Software version 1.1 (Beckman Coulter, Inc., Brea, CA). For cell sorting, the mouse anti-rat integrin α6β1 antibody and a goat anti-integrin α3 antibody were used. The anti-integrin antibodies were labeled with Alexa488-conjugated donkey anti-mouse IgG (H+L) and Alexa633-conjugated donkey anti-goat IgG (H+L). Cells were incubated with each antibody for 30 minutes and then washed with Wash Buffer. After the cells had been stained with propidium iodide, they were sorted based on the expression levels of integrin α6β1 and α3 by using a FACS Aria cell sorter (BD Biosciences). Integrin $\alpha3^{high}\alpha6\beta1^{high}$, $\alpha3^{low}\alpha6\beta1^{high}$, or $\alpha3^{low}\alpha6\beta1^{low}$ cells were plated on LN111-coated 24-well plates and cultured for 28 days.

Inhibition assay using neutralizing antibodies

First-passage cells that had been cultured on the Matrigel-coated dishes for 28 days were collected by trypsinization. For the study of integrin β1 dependence, the cells were incubated for 2 hours on ice in hamster anti-rat integrin β1 IgM antibody (20 μg/mL) or hamster IgM isotype one as a control. After washing with PBS, the cells were suspended in the medium

and plated and cultured on LN111-, LN511-, and Matrigel-coated 12-well plates. The rates of cell attachment and colony formation were assessed at days 1 and 7, respectively. For the study of LN111 dependence, the cells were washed in PBS, suspended in medium containing rabbit anti-LN111 antibody (5 μg/mL), and plated on LN111-, LN511-, and Matrigel-coated 12-well plates. Goat anti-rabbit IgG (5 μg/mL) was used as a control. After 1 day of culture, the medium was replaced with medium lacking antibodies. The rates of cell attachment and colony formation were assessed at days 1 and 7, respectively.

Supporting Information Legends

Supporting TABLE S1. List of primers used in the experiments of gene expression analyses using (A) real-time PCR and (B) RT-PCR.

Supporting TABLE S2. List of antibodies used in the experiments.

Supporting TABLE S3. Properties of the colonies formed on Matrigel, LN111, or LN511. The first-passage cells were trypsinized and plated onto Matrigel-, LN111-, or LN511 (E8 fragment)-coated 12-well plates. The cells were fixed 7 days after plating. To measure the labeling index, the cells were treated with 5-bromo-2′-deoxyuridine (BrdU) for 18 hours before fixation. The sizes of colonies and the cells in the colonies were measured by counting the numbers of cells and colonies in photomicrographs. Asterisks (*) represent significant differences ($P < 0.05$).

Supporting Figures

Supporting FIG. S1. (A) To examine the concentration dependence of cell attachment on LN111, first-passage cells were plated on 12-well plates coated with LN111. Attached cells were counted 1 day after plating. The data were analyzed by analysis of variance (ANOVA) with Tukey's multiple comparison test. Asterisks (*) represent significant differences ($P < 0.05$). Bars depict means ± SEM of three wells. (B) To examine the difference between LN 511 E8 fragment (LN511-E8) and full-length LN511 (LN511-FL) regarding cell attachment and the effect of anti-LN111 and anti-integrin β1 neutralizing antibodies, first-passage cells (75,000 cells/well) were plated on 12-well plates. Attached cells were counted 1 day after plating. Bars depict means ± SEM of three wells.

Supporting FIG. S2. (A) The sizes of the cells on Matrigel (Mat)-, LN111-, LN511 (E8 fragment)-, and LN-521-coated 12-well plates were measured 1 day after plating. The sizes of the cells are plotted, and the bars show the means of all cells counted. The data were analyzed by ANOVA with Tukey's multiple comparison test. Asterisks (*) represent significant differences ($*P < 0.05$). (B) Phase-contrast images of the second-passage cells on LN521-coated 12-well plates 3 hours, 1 day, and 7 days after plating. Scale bar: 200 μm.

Supporting FIG. S3. (A) LN-subtype-dependent adhesion of first-passage cells. An overview of the procedure. To show that two different populations are present in the first-passage cells cultured on Matrigel, these cells were collected after 21 days of culture and plated on LN111-coated dishes. Three hours after plating, culture medium containing unattached cells was collected and transferred to LN511 (E8 fragment)-coated dishes. The cells were cultured for a further hour and then harvested. Total RNA was isolated, and gene expression was analyzed. The cells on Matrigel were used as a control. (B) LN-subtype-dependent adhesion of first-passage cells. Phase-contrast images of a representative colony before passage and cells 4 hours and 7 days after plating on Matrigel, LN111, and LN511 (E8 fragment). Many cells that did not attach to LN111 could attach on LN511 at 1 hour after plating. At day 7, a typical HPPC colony was observed on LN111, whereas colonies consisting of large-sized cells were observed on LN511. On Matrigel, both types of colonies were observed. Scale bars: 100 μm.

Supporting FIG. S4. The passage cells cultured on LN111-coated dishes retained the ability to self-renew without losing hepatic function. CD44-positive cells were expanded in hyaluronic acid-coated dishes, subcultured 9 days after plating, and plated onto LN111-coated dishes. The cells were cultured for 28 days and then passaged. The collected cells were replated onto fresh

LN111-coated dishes. Rock inhibitor (10 μM Y-27632) was added to the medium at replating. One day after plating, culture medium was replaced with fresh medium lacking Y-27632 and then replenished every other day. (A) Phase-contrast images taken at the time of passage. (B) RT-PCR analysis of aliquots of the cells collected at each passage.

Supporting FIG. S5. Differences in the expression of genes related to hepatic function and stem cells among the cells attached on Matrigel, LN111, and LN511 (E8 fragment). The cells on Matrigel-, LN111-, or LN511-coated dishes, which are described in Fig. 2, were analyzed by qPCR. Mature hepatocytes (MHs) were analyzed as a reference. Bars depict means ± SEM of three samples. N.D.; not determined.

Supporting FIG. S6. (A) Expression of laminin subunit genes was analyzed by RT-PCR; primary hepatocytes (MH), small hepatocytes (SHs) sorted by anti-CD44-Ab (CD44-positive), and second-passage cells attached to LN111, LN511 (E8 fragment), or Matrigel at 4 hours after passage. (B) Expression of genes related to ECM in the cells attached on Matrigel, LN111, and LN511 was analyzed by oligo microarrays. The samples are the same as those shown in Figs. 2 and 3.

Supporting FIG. S7. Expression of genes related to hepatic functions and stem cells in second-passage cells with or without Matrigel overlay (MGOL) was analyzed using qPCR. The second-passage cells were cultured on LN111-, LN511 (E8 fragment)-, and Matrigel-coated dishes for 14 days, after which the medium was replaced with a medium containing or lacking 5% Matrigel for 7 days. All data were analyzed using Kruskal–Wallis ANOVA with Dunn's multiple comparison test. Asterisks (*) represent significant differences ($*P < 0.05$). Bars represent means ± SEM of three dishes.

Supporting TABLE S1 List of primers used in the experiments of gene expression analyses.

(A) Real-time PCR primers

Genes	Real-Time PCR Primers
Albumin	Rn00592480_m1
Hnf4a	Rn00573309_m1
Cebpa	Rn00560963_s1
Tat	Rn01640359_m1
Tdo2	Rn00574499_m1
Cyp1a2	Rn01457875_m1
Itga3	Rn01751608_m1
Itga6	Rn01512708_m1
Itga7	Rn01529354_m1
Itgb1	Rn00566727_m1
Itgb4	Rn00566017_m1
Cd44	Rn00681157_m1
Cd24	Rn00562598_m1
Krt19	Rn01496867_m1
Sox9	Rn01751069_m1
Epcam	Rn01473202_m1
Afp	Rn00560661_m1
Thy1	Rn00562048_m1
c-Kit	Rn00573942_m1
Gapdh	Rn01775763_g1

(B) RT-PCR primers

Genes	RT-PCR Primers
Itga1	AGG CTT CTG CGT CTC CTT CAA TGT GCT TAG GGC CAA TAT CCA TCC TCT
Itga2	ATG TGC TCT TGG TAG GTG CTC C TGA TGT CCA CTC GCA GAT CCA AAG
Itga3	GAT GAT GAC TAC ACC AAC CGG ACT TGC CAC CCA TCA TTG TTC AGG TCT
Itga4	TCC CAG GCT ACA TCG TTT TG GCT CCC AAC AGC AAG ATA GG
Itga5	TAT GCC GTA GCT GCC ACT GAT AC GCA GAA GCT AAG GTT GAT GCA GGA
Itga6	TGA TAT GGA TGG AGG AGA CTG GAG CAC ATT ACT CCA TCT GCC TTG CTG
Itga7	TTG GAT GGT GGG GAG TGG AAG TT ACA TAC ACG GCA CCT CCA AGT TCT
Itgav	TTG GCA GGG TCA GCT CAT TTC AGA AAG GCC AGC ATT TAC GGT GAC AAC
Itgb1	GGT TTC ACT TTG CTG GAG ATG GGA CGT TGG ACC TAT CGC AGT TGA AGT
Itgb2	CAG CCG ATG ATA TAA TGG ACC CC AGC TGG ACT ACG TTA CTG GAA TCG
Itgb3	AAAGTGGAGCTGGAAGTGCGTGAT CAG TTC TTT CAC CAG CTC GAT GTC
Itgb4	GTA ACA TCC ACC TGA AAC CCT CCT CCA CCA CCT CTT CCG CTT TCT TAA
Itgb5	ACT ATC CAT CGC TTG CCT TGC TTG ACT TCT CAC ACG TCT CCC CAA AG
Itgb6	CACCAGAGGAAATCACCAACCCTT CTG TAT CTC CGA CTT TCA TGT GGG
Lama1	ACC AGA GAA CGG AGT GAG AC GTG GGG CTG AAA CTG AAA GG
Lama2	TTG AAG GGA AAA AGT TGA TGG C ACT CGG TAA AAT CCT GGT GC
Lama3	CAG GAG GCA GTT ATG GAC CG GGT TGA GTA GGG ATG CGA GC
Lama4	AGA GCC GAC GCA AAC AAC GGC AAA CTG GGA TTT TTC ACC
Lama5	ACA GCA TCA AAG ACA TCA GCA TCG GCT CGC AGT TGA TAC CCG TG
Lamb1	GGC AAT CGG AAA ATG GTG TG AA GGT TAT CTC CCA AGG TGT G
Lamb2	GGA CAC AAT CCT GGC ACA TAC C AAC ACC TTC AGC CTT CCG TTC
Lamb3	ATG AGT GCC AAA GGT GTG ACT CAA GCA GCG TCC AGT TTC C
Lamc1	GCT GGT GAA GGA TAA GGT TGC GGT CTC GTT GGC TGT CTT TG
Lamc2	GCC ACT CAA AAG GTT CCC TC GCG GTA GTC AAA AGA CAG GC
Lamc3	TGG ACT GTG AGC GTT GTC TAC C TGA GCG GAT GTG GTG TTC CTG
Alb	AAG GCA CCC CGA TTA CTC CG

	TGC GAA GTC ACC CAT CAC CG
Krt19	ATG ACT TCC TAT AGC TAT CG CAC CTC CAG CTC GCC ATT AG
Cd44	TCC CAC TAT GAC ACA TAT TGC ACA CCT TCT CCT ACT GTT GAC
Gapdh	ACC ACA GTC CAT GCC ATC AC TCC ACC ACC CTG TTG CTG TA

1
2

Supporting TABLE S2. List of antibodies used in the experiments.

Antibodies	Host	Supplier	Dilution
CD44	Mouse	BD Biosciences Pharmingen, Franklin Lakes, NJ (cat. no. 554869)	1:1000
HNF4α	Rabbit	Santa Cruz, Santa Cruz, CA (cat. no. sc-6556)	1:200
Albumin	Goat	MP Biomedicals, LLC-Cappel Products, Santa Ana, CA (cat. no. 55727)	1:800
BrdU	Mouse	DakoCytomation, Glostrup, Denmark (cat. no. M0744)	1:200
Laminin111	Rabbit	Sigma-Aldrich, St Louis, MO (cat. no. L9393)	1:100
Anti-rabbit IgG	Goat	Sigma-Aldrich, St Louis, MO (cat. no. R5506)	1:100
Integrin α6β1	Mouse	CHEMICON, Temecula, CA (cat. no. MAB1410)	1:1600
Integrin α3	Mouse	BD Biosciences Pharmingen, Franklin Lakes, NJ (cat. no. 611044)	1:200
Integrin α3	Goat	R&D Biosystems, Inc., Minneapolis, MN (cat. no. AF2787)	1:200
Integrin β1	Hamster	BD Pharmingen, Franklin Lakes, NJ (cat. no. 555002)	1:50
IgM isotype control	Hamster	BD Pharmingen, Franklin Lakes, NJ (cat. no. AB1922)	1:50
Integrin β4	Rabbit	CHEMICON, Temecula, CA (cat. no. 553957)	1:1600
Mouse IgG2a+b microbeads	Rat	Miltenyi Biotec, Bergisch Gladbach, Germany (cat. no. 130-047-201)	1:5
Alexa 488-conjugated anti-mouse	Goat	Molecular Probes, Eugene, OR (cat. no. A11029)	1:500
Alexa 488-conjugated anti-mouse	Rabbit	Molecular Probes, Eugene, OR (cat. no. A11059)	1:500
Alexa 594-conjugated anti-mouse	Goat	Molecular Probes, Eugene, OR (cat. no. A11005)	1:500
Alexa 488-conjugated anti-rabbit	Donkey	Molecular Probes, Eugene, OR (cat. no. A21206)	1:500
Alexa 555-conjugated anti-mouse	Donkey	Molecular Probes, Eugene, OR (cat. no. A31570)	1:500
Alexa 555-conjugated anti-rabbit	Donkey	Molecular Probes, Eugene, OR (cat. no. A31572)	1:500
Alexa 594-conjugated anti-rabbit	Donkey	Molecular Probes, Eugene, OR (cat. no. A21207)	1:500
Alexa 594-conjugated anti-goat	Donkey	Molecular Probes, Eugene, OR (cat. no. A11058)	1:500
Alexa 633-conjugated anti-goat	Donkey	Molecular Probes, Eugene, OR (cat. no. A21082)	1:200
Biotin-conjugated anti-mouse	Horse	Vector Laboratories, Burlingame, CA (cat. no. BA-2000)	1:200

Supporting TABLE S3. Properties of the colonies formed on Matrigel, LN111, or LN511

	Matrigel	LN111	LN511
Colony size (cells/colony)	22.22 ± 13.8	32.53 ± 26.15*	19.87 ± 9.12
Labeling index	13.50 ± 6.15	13.10 ± 7.90	22.22 ± 13.8
Cell size ($\times 10^3$ μm^2)	1.82 ± 0.52	1.53 ± 0.46*	2.04 ± 0.42

*$P < 0.05$ (vs LN511)

Figure S1

A

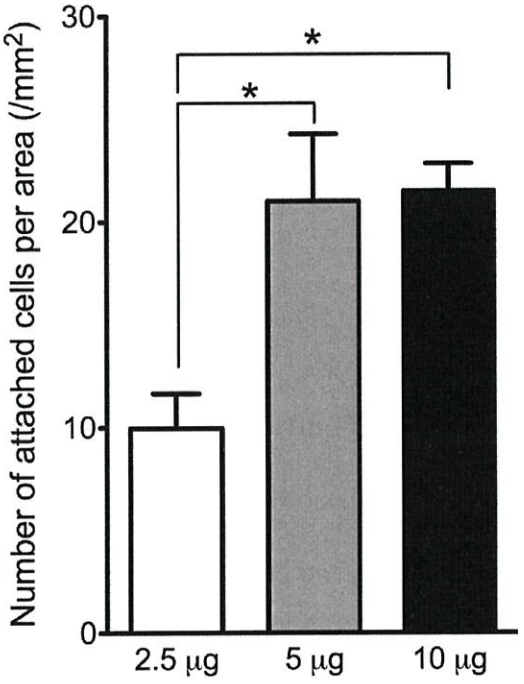
Number of attached cells per area (/mm2)
30
20
10
0
*
*
2.5 μg
5 μg
10 μg

B

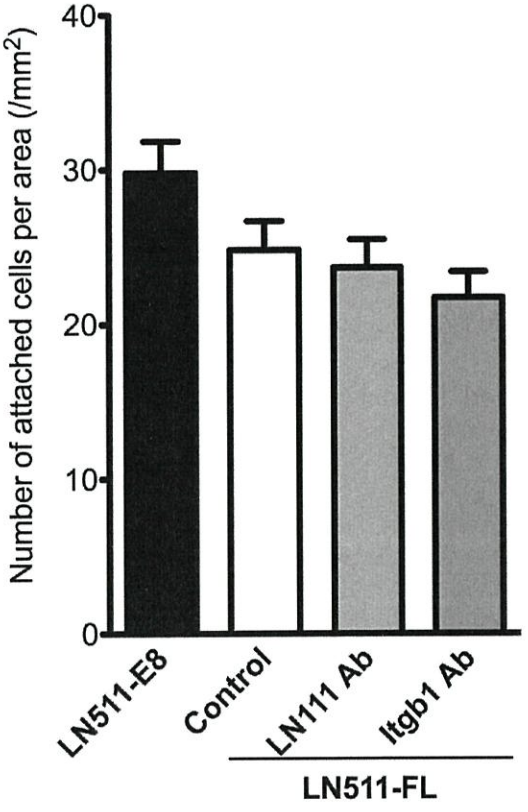
Number of attached cells per area (/mm2)
40
30
20
10
0
LN511-E8
Control
LN111 Ab
Itgb1 Ab
LN511-FL

A

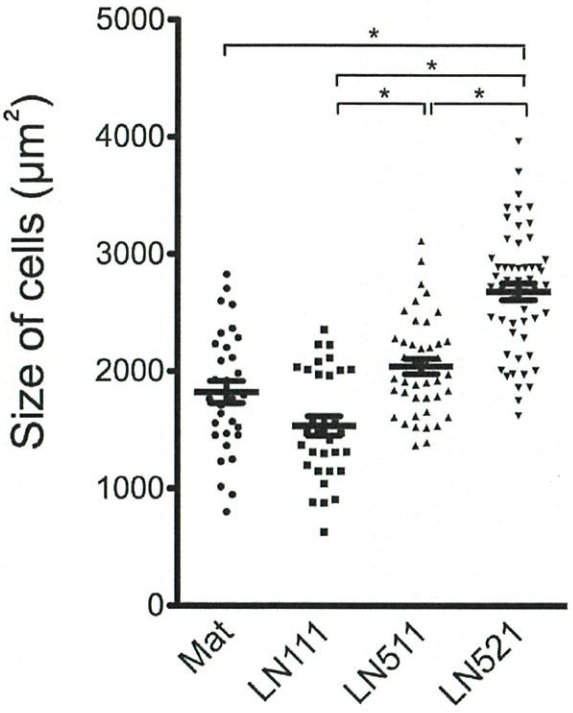
Size of cells (µm²)
5000
4000
3000
2000
1000
0
*
*
*
*
Mat
LN111
LN511
LN521

B

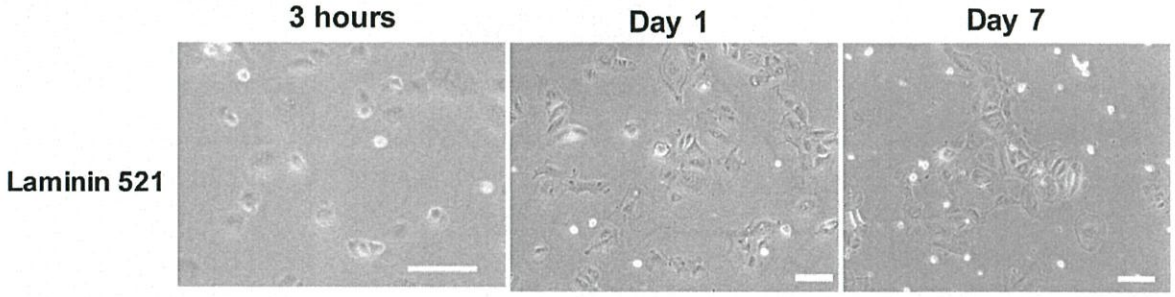
3 hours
Day 1
Day 7
Laminin 521

1

2

Figure S3

A

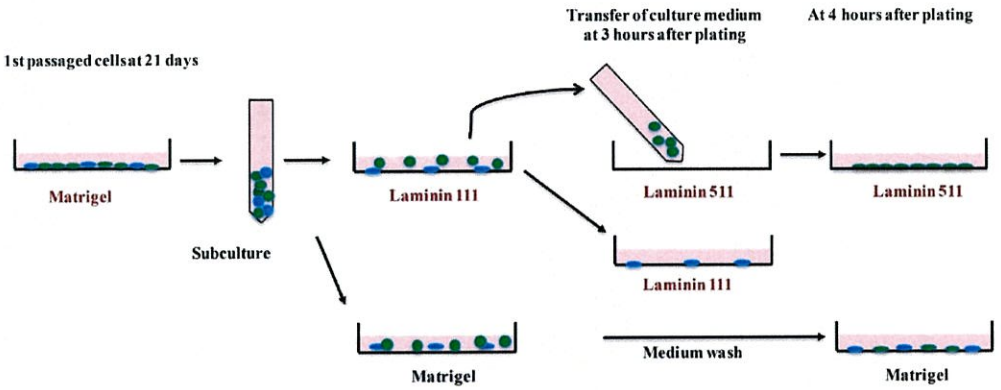
1st passaged cells at 21 days
Matrigel
Subculture
Laminin 111
Transfer of culture medium at 3 hours after plating
Laminin 511
At 4 hours after plating
Laminin 511
Laminin 111
Matrigel
Medium wash
Matrigel

B

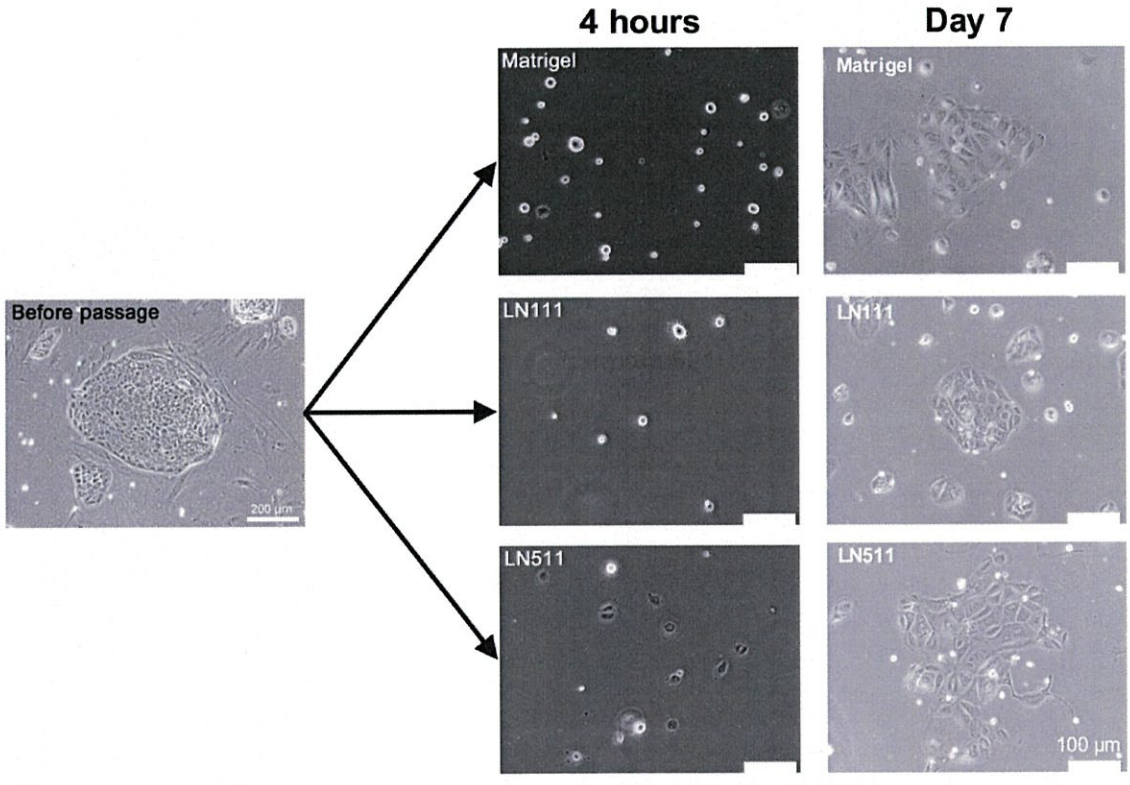
4 hours
Day 7
Before passage
200 μm
Matrigel
Matrigel
LN111
LN111
LN511
LN511
100 μm

Figure S4

A

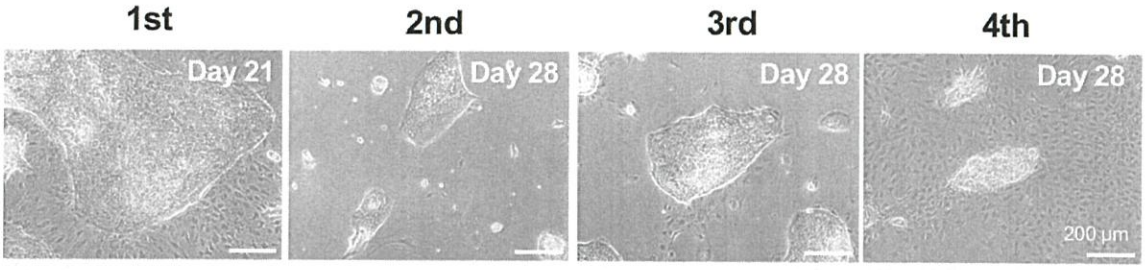

B

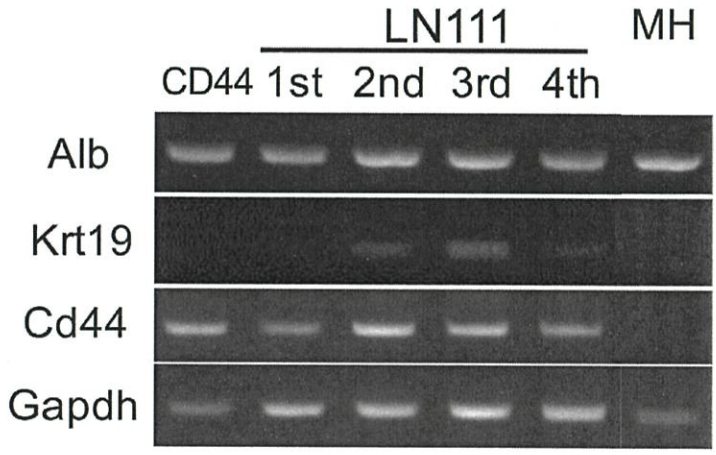

1

2

Figure S5

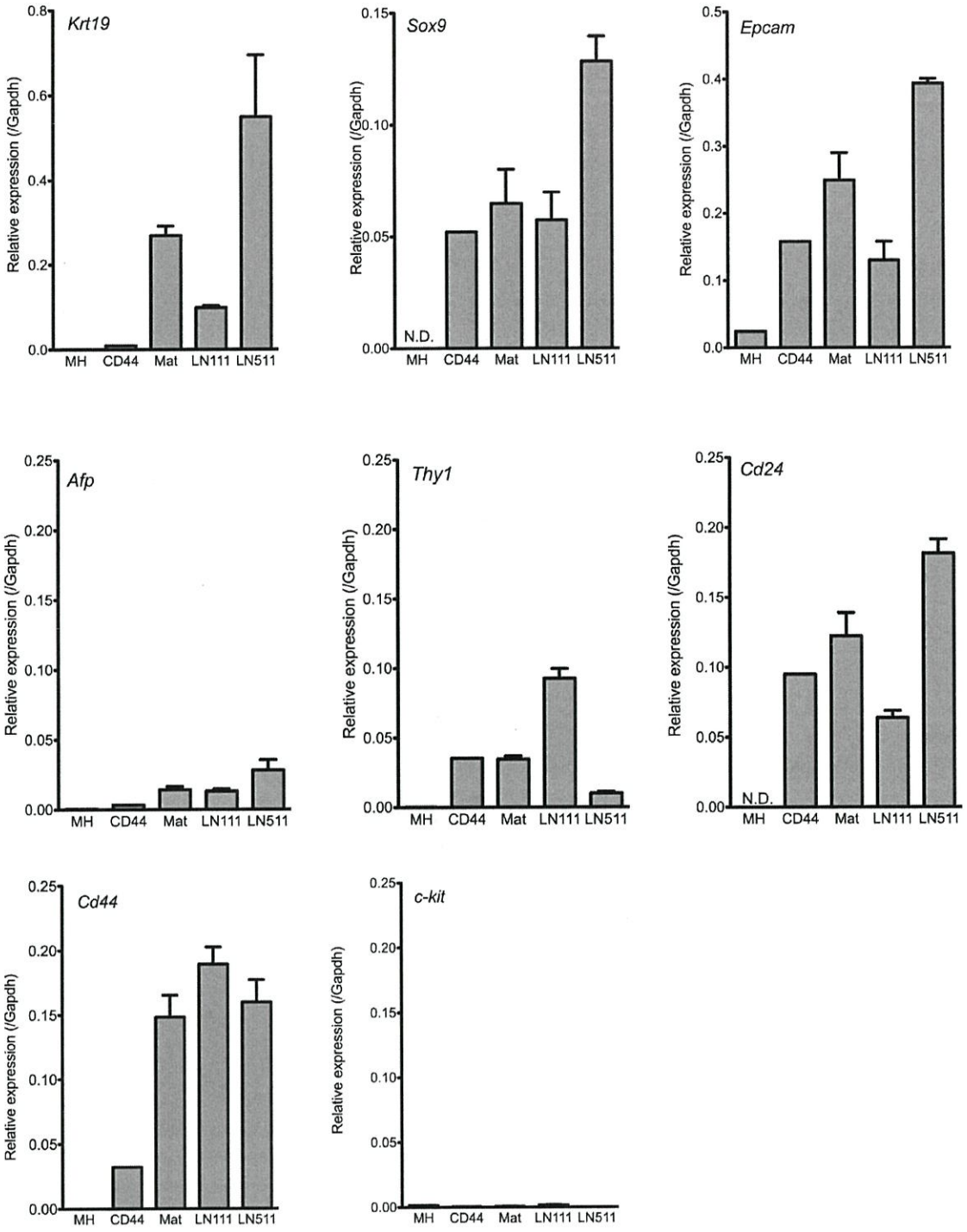
Krt19
Sox9
Epcam
Afp
Thy1
Cd24
Cd44
c-kit
Relative expression (/Gapdh)
N.D.
MH
CD44
Mat
LN111
LN511

Figure S6

A

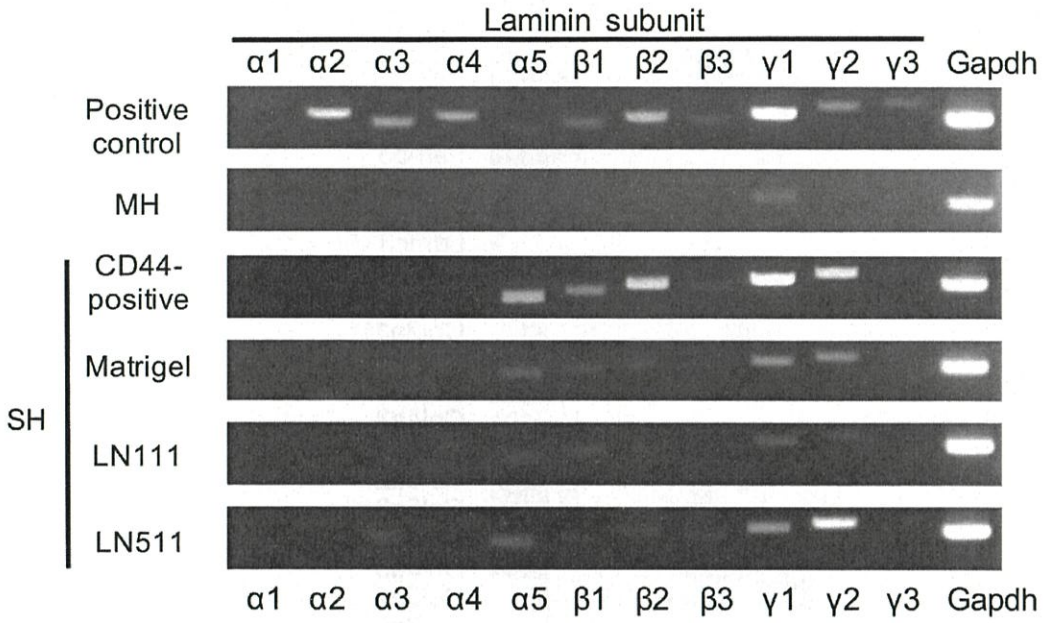
Laminin subunit
α1 α2 α3 α4 α5 β1 β2 β3 γ1 γ2 γ3 Gapdh
Positive control
MH
SH
CD44-positive
Matrigel
LN111
LN511
α1 α2 α3 α4 α5 β1 β2 β3 γ1 γ2 γ3 Gapdh

Figure S6

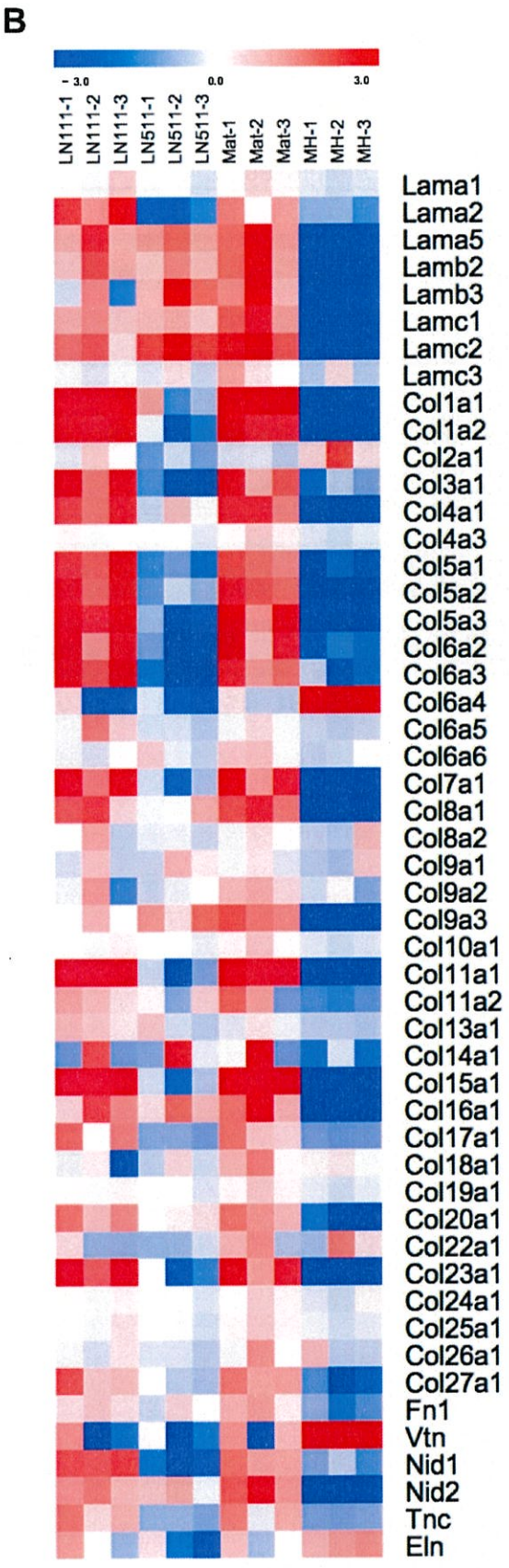
B
- 3.0
0.0
3.0
LN111-1
LN111-2
LN111-3
LN511-1
LN511-2
LN511-3
Mat-1
Mat-2
Mat-3
MH-1
MH-2
MH-3
Lama1
Lama2
Lama5
Lamb2
Lamb3
Lamc1
Lamc2
Lamc3
Col1a1
Col1a2
Col2a1
Col3a1
Col4a1
Col4a3
Col5a1
Col5a2
Col5a3
Col6a2
Col6a3
Col6a4
Col6a5
Col6a6
Col7a1
Col8a1
Col8a2
Col9a1
Col9a2
Col9a3
Col10a1
Col11a1
Col11a2
Col13a1
Col14a1
Col15a1
Col16a1
Col17a1
Col18a1
Col19a1
Col20a1
Col22a1
Col23a1
Col24a1
Col25a1
Col26a1
Col27a1
Fn1
Vtn
Nid1
Nid2
Tnc
Eln

1

Figure S7

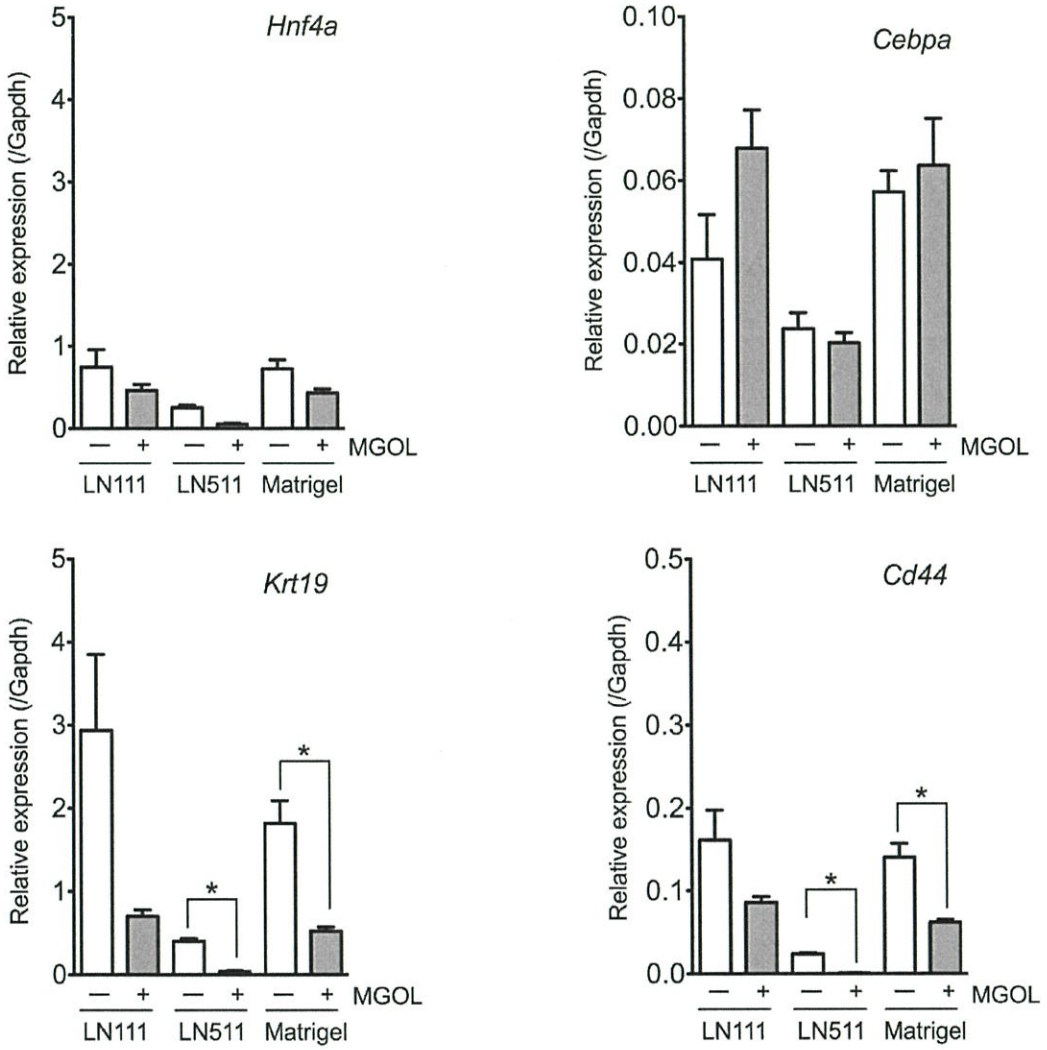

2

3